

OPTIMIZATION OF SURFACTANT MIXTURES AND THEIR
INTERFACIAL BEHAVIOR FOR ADVANCED OIL RECOVERY

Annual Report
January 15, 2001

By:
Prof. P. Somasundaran

Date Published: April 2001

Work Performed Under Contract No. DE-AC26-98BC15112

Columbia University in the city of New York
New York, New York



**National Energy Technology Laboratory
National Petroleum Technology Office
U.S. DEPARTMENT OF ENERGY
Tulsa, Oklahoma**

DISCLAIMER

This report was prepared as an account of work sponsored by an agency of the United States Government. Neither the United States Government nor any agency thereof, nor any of their employees, makes any warranty, expressed or implied, or assumes any legal liability or responsibility for the accuracy, completeness, or usefulness of any information, apparatus, product, or process disclosed, or represents that its use would not infringe privately owned rights. Reference herein to any specific commercial product, process, or service by trade name, trademark, manufacturer, or otherwise does not necessarily constitute or imply its endorsement, recommendation, or favoring by the United States Government or any agency thereof. The views and opinions of authors expressed herein do not necessarily state or reflect those of the United States Government.

This report has been reproduced directly from the best available copy.

Optimization of Surfactant Mixtures and Their Interfacial Behavior for Advanced Oil Recovery

By
Prof. P. Somasundaran

April 2001

Work Performed Under Contract DE-AC26-98BC15112

Prepared for
U.S. Department of Energy
Assistant Secretary for Fossil Energy

Jerry F. Casteel, Technology Manager
National Petroleum Technology Office
P.O. Box 3628
Tulsa, OK 74101

Prepared by
Columbia University in the city of New York
Box 20, Low Memorial Library
New York, NY 10027

TABLE OF CONTENTS

	Page
LIST OF FIGURES	v
LIST OF TABLES	vii
EXECUTIVE SUMMARY	ix
MATERIALS & METHODS	1
MATERIALS	1
Surfactants:	1
Mineral Samples	2
Other Chemicals	2
METHODS	3
Surface tension	3
Adsorption experiments	3
Desorption	3
Analytical Techniques	3
Electrokinetics	4
Calcium Ion Measurement	4
FTIR Spectroscopy	4
RESULTS & DISCUSSION	5
I. Adsorption Mechanism of n-dodecyl- β -D-maltoside on Alumina	5
1. Adsorption/Desorption of n-dodecyl- β -D-maltoside on alumina	5
2, Effect of pH on the adsorption of n-dodecyl- β -D-maltoside on alumina	7
3. Zeta-potential of alumina after n-dodecyl- β -D-maltoside adsorption	7
4. Interaction between calcium ion and n-dodecyl- β -D-maltoside	8
5. Adsorption of maltose on alumina	10
6. Effect of temperature on adsorption of n-dodecyl- β -D-maltoside on alumina	11
7. Adsorption/desorption of n-dodecyl- β -D-maltoside on alumina in urea and DMSO solutions	12

8. Characterization of N-Dodecyl- β -D-Maltoside/Alumina Interactions by FTIR Spectroscopy	13
II. Surface Tension of Sugar-based Surfactants with Anionic Surfactant	17
1. Surface tension of n-dodecyl- β -D-maltoside and sodium dodecylsulfate mixtures ..	17
2. Surface tension of dodecyl polyglucoside and sodium dodecylsulfate mixtures ...	20
III. Adsorption of Sugar-based Surfactants along with Anionic Surfactant at pH 6	21
1. Adsorption of dodecyl polyglucoside/sodium dodecylsulfate and n-dodecyl- β -D-maltoside/sodium dodecylsulfate 1:1 mixtures	21
2. Adsorption of n-dodecyl- β -D-maltoside/sodium dodecylsulfate 3:1 and 1:3 mixtures	23
3. Adsorption of dodecyl polyglucoside/sodium dodecylsulfate mixtures	28
4. Summary of sugar-based surfactant/SDS mixtures adsorption at pH 6	29
III. Adsorption of Sugar-based Surfactants with Anionic Surfactant at pH 11	30
1. Adsorption of dodecyl polyglucoside/sodium dodecylsulfate and n-dodecyl- β -D-maltoside/sodium dodecylsulfate mixtures	30
2. Summary of sugar-based surfactant/SDS mixtures adsorption at pH 11	35
V. Theoretical And Experimental studies of the Adsorption of Surfactant at Interfaces	36
1. Description Of The Model	36
2. Mathematical Formulation	37
3. Experiments	38
PUBLICATION	43

LIST OF FIGURES

	Page
Figure 1. The Chemical Structures of a) n-dodecyl- β -D-maltoside, and b) dodecyl polyglucosides	1
Figure 2. Adsorption and Desorption Isotherms of n-Dodecyl- β -D-Maltoside on Alumina ...	6
Figure 3. Effect of pH on the Adsorption of n-Dodecyl- β -D-Maltoside on Alumina	7
Figure 4. Zeta-potential of Alumina after n-Dodecyl- β -D-Maltoside Adsorption at Neutral pH	8
Figure 5. Effect of n-Dodecyl- β -D-Maltoside on the Calcium Conductivity	9
Figure 6. Adsorption of Maltose on Alumina Compared with that of n-Dodecyl- β -D-Maltoside	10
Figure 7. Effect of Temperature on the Adsorption of n-Dodecyl- β -D-Maltoside on Alumina	11
Figure 8. Adsorption and Desorption of n-Dodecyl- β -D-Maltoside in the Presence of 5M Urea	12
Figure 9. Adsorption and Desorption of n-Dodecyl- β -D-Maltoside in the Presence of 85% DMSO	13
Figure 10 A) 4000-400 cm^{-1} ATR Spectrum of DM Adsorbed on Alumina with Alumina Subtracted(a), Compared to the Spectrum of DM in Solution (b)	14
Figure 10 B) 1200-800 cm^{-1} ATR Spectrum of DM Adsorbed on Alumina with Alumina Subtracted(a), Compared to the Spectrum of DM in Solution (b)	15
Figure 11. ATR Spectrum of Maltose Adsorbed on Alumina with Alumina Subtracted(a), Compared to the Spectrum of Maltose in Solution (b)	16
Figure 12. Surface Tension vs. Concentration of DM/SDS Mixed Surfactant System Without Salt	19
Figure 13. Surface Tension vs. Concentration of DM/SDS Mixed Surfactant System With Salt	19
Figure 14. The Surface Tension vs. Concentration of C12APG/SDS Mixed Surfactant System With Salt	20

Figure 15.	Adsorption of DM, SDS and DM/SDS 1:1 Mixture on Alumina	22
Figure 16.	Adsorption of C ₁₂ -APG, SDS and C ₁₂ -APG/SDS 1:1 Mixture on Alumina	23
Figure 17.	Adsorption of DM, SDS and their 3:1, 1:1 and 1:3 Mixtures on Alumina	24
Figure 18.	Adsorption of SDS on Alumina: Adsorption for SDS alone and from DM/SDS 3:1, 1:1 and 1:3 Mixtures	25
Figure 19.	Adsorption of DM on Alumina: Adsorption for DM alone and from DM/SDS 3:1, 1:1 and 1:3 Mixtures	25
Figure 20.	Adsorption of DM/SDS Mixtures and the DM/SDS ratios in the Adsorption Layer A) 1:3; B) 1:1; C) 3:1	27
Figure 21.	Adsorption of APG alone and from APG/SDS 1:1 Mixture on Alumina	28
Figure 22.	Adsorption of SDS alone and from APG/SDS 1:1 Mixture on Alumina	29
Figure 23.	Adsorption of n-dodecyl-β-D-maltoside(DM), sodium dodecyl sulfate (SDS) and C ₁₂ -APG/SDS 1:1 Mixtures on Alumina at pH 11	30
Figure 24.	Adsorption of dodecyl polyglucosides(C12-APG), sodium dodecyl sulfate (SDS) and C ₁₂ -APG/SDS 1:1 Mixtures on Alumina at pH 11	31
Figure 25.	Adsorption of DM, SDS and their 3:1, 1:1 and 1:3 Mixtures on Alumina at pH 11	32
Figure 26.	Adsorption of SDS on Alumina at pH 11: Adsorption for SDS alone and from DM/SDS 3:1, 1:1 and 1:3 Mixtures	32
Figure 27.	Adsorption of DM on Alumina at pH 11: Adsorption for DM alone and from DM/SDS 3:1, 1:1 and 1:3 Mixtures	33
Figure 28.	Adsorption of APG alone and in APG/SDS 1:1 mixture on alumina at pH 11	34
Figure 29.	Adsorption of SDS alone and in APG/SDS 1:1 mixture on alumina at pH 11	34
Figure 30.	Surface tension of C ₁₄ E ₆ solution (5.965 * 10 ⁻⁶ M)as a function of time	40
Figure 31.	Surface tension of C ₁₄ E ₆ solution (1.927 * 10 ⁻⁵ M)as a function of time	40
Figure 32.	Surface tension of C ₁₄ E ₆ solution (3.911 * 10 ⁻⁵ M)as a function of time	41
Figure 33.	Surface tension of C ₁₄ E ₆ solution (7.719 * 10 ⁻⁵ M)as a function of time	41
Figure 34.	Surface tension of C ₁₄ E ₆ solution (9.666 * 10 ⁻⁵ M)as a function of time	42

LIST OF TABLES

	Page
Table I. Surfactants used and their molecular structure	2
Table 2 Results of Surface Tension Data Analysis for DM/SDS Mixtures Without Salt at 25°C	18
Table 3 Results of Surface Tension Data Analysis for DM/SDS Mixtures With Salt at 25°C	18
Table 4. Summary of Figures 30 - 34	39

EXECUTIVE SUMMARY

The aim of this research project is to develop improved extraction processes to mobilize and produce the oil left untapped using conventional techniques. Current chemical schemes for recovering the residual oil have been in general less than satisfactory. High cost of the processes as well as significant loss of chemicals by adsorption on reservoir minerals and precipitation has limited the utility of chemical-flooding operations. There is a need to develop cost-effective, improved reagent schemes to increase recovery from domestic oil reservoirs. It is our aim to develop and evaluate novel mixtures of surfactants for improved oil recovery. Emphasis will be placed on designing cost-effective processes compatible with existing conditions and operations in addition to ensuring minimal reagent loss. The advantage of using surfactant mixtures is that interfacial behavior of such mixtures can be synergistic (or antagonistic) and can be manipulated by adjusting surfactant type and properties, such as mixing ratio and the order of addition. It is to be noted that the past fundamental work in these systems has been mostly using single surfactants while commercial systems invariably are mixture.

During the second year of this project, the interfacial behavior of sugar-based surfactants has been studied both in solutions and at solid-liquid interfaces. Sugar-based surfactants, alkyl polyglucosides, comprise a class of biodegradable surface active agents that are environmentally benign. Based on the information provided by our industrial collaborators in the oil industry, due to their high surface activity and better salinity and temperature tolerance, this type of surfactants has some potential for replacing currently used surfactants in oil recovery.

In the last annual report, adsorption of alkyl glucosides and alkyl maltosides on various solids has been discussed. During this reporting period, adsorption of sugar-based n-dodecyl- β -D-maltoside on alumina has been studied in more detail to reveal the mechanisms of adsorption. Through systematic studies, it was concluded that neither electrostatic interaction nor chemical interaction is the single governing force for the adsorption of n-dodecyl- β -D-maltoside on this oxide. The adsorption isotherm of n-dodecyl- β -D-maltoside on alumina has a relatively small slope in the low concentration range, indicating weak driving force for adsorption. The sharp increase in adsorption density at higher concentrations is attributed to the hydrophobic chain-chain interactions. This is indicated by the concave shape of the isotherm. It is therefore proposed that hydrogen bonding between hydroxyl groups on the surfactants and alumina surface hydroxyl species is the primary force for the adsorption of alkyl polyglucosides on alumina. This has been verified by studying the adsorption/desorption of this surfactant in the presence of urea and DMSO(dimethyl sulfoxide), both hydrogen bond breakers, and FTIR analysis.

During this reporting period, the adsorption of nonionic-anionic mixtures of dodecyl polyglucosides (C12-APG) and sodium dodecyl sulfate (SDS), as well as n-dodecyl- β -D-maltoside (DM) and sodium dodecyl sulfate (SDS), at liquid-air and solid-liquid interfaces was studied under different pH conditions. This is done as a part of our effort to explore possible synergism or antagonism between the two surfactants under various conditions, and to compare the behavior of commercial sugar-based surfactants with laboratory counterparts. This has important implications for the use of mixed surfactant systems in enhanced oil recovery.

The interactions of sugar-based dodecyl polyglucosides (C12-APG) and n-dodecyl- β -D-

maltoside (DM) with sodium dodecyl sulfate (SDS), was first studied with and without a supporting electrolyte in the solution. As they all have the same hydrophobic chain length, any deviation from ideality can be ascribed to dissimilarity in the hydrophilic headgroups. For DM/SDS system, the average interaction parameter β is -3.67 without salt and -2.89 with, indicating strong interaction between them. For C12-APG/SDS, the interaction parameter is -3.20. This β value is typical of nonionic-ionic mixed surfactant systems. The synergy is due to the decrease in the surface charge density of the micelles and the steric repulsion. The presence of salt is found to reduce the synergy between the surfactants. The interaction parameter of DM/SDS is reduced from -3.67 in water to -2.89 in 0.03M NaCl. This is mainly due to charge neutralization by the sodium counterions. Similarity in interactions between DM/SDS and APG/SDS implies that commercial polyglucosides are similar to pure laboratory samples in synergistic interactions with the anionic surfactant, suggesting that the pure alkyl polyglucosides may be used for studying interactions of sugar-based surfactants in general.

Co-adsorption of n-dodecyl- β -D-maltoside (DM) and dodecyl polyglucosides (C₁₂-APG) on alumina from its mixtures with anionic sodium dodecyl sulfate (SDS) was investigated at pH 6 where alumina is positively charged and pH 11 where it is negatively charged. At pH 6, marked synergistic effects between DM/APG and SDS were observed, especially in the region where hydrophobic chain-chain interaction dominates the adsorption process as long as the surface is not saturated. In the plateau region, clearly there is competition for adsorption sites. At this pH, SDS and DM/APG promote adsorption of each other and there exists mainly synergism. The strongest synergism was found when DM:SDS was 1:1. At pH 11, the adsorption of APG/SDS, or DM/SDS mixture is less than those of APG or DM alone. The presence of SDS in the systems reduces the sugar-based surfactants adsorption except in the rising part,

although the SDS adsorption itself is increased due to hydrophobic interaction with sugar-based surfactants. Generally there is mainly antagonistic effect between DM/APG and SDS at this pH. Since weak adsorption of surfactants is essential for them to be cost effective in chemical flooding operations for enhanced oil recovery (EOR), these results have useful implications for the oil industry.

A theoretical model for the adsorption of surfactant molecules at the air-liquid and solid-liquid interfaces both below and above the critical micelle concentration has been developed. This model was developed for the kinetics of surfactant adsorption i.e., surfactant adsorption from the bulk solution as a function of time, to an initially clean interface above the critical micelle concentration (CMC). The model can be applicable to both solid-liquid and air-liquid interfaces. At the air-liquid interface, the surface concentration is related to the surface tension using the equation of state. In order to test this model, dynamic surface tension of $C_{14}E_6$ solutions above the CMC has been measured using a pendant bubble setup. The experiment results are compared with theoretical predictions.

In general, during this reporting period, adsorption mechanisms of n-dodecyl- β -D-maltoside on alumina have been explored and hydrogen bond is proposed to be the driving force for adsorption. Mixtures of sugar-based surfactants and sodium dodecyl sulfate show synergy in solution that is similar to that of other nonionic-anionic mixtures. However, at solid-liquid interface, depending on solution pH, the sugar-based surfactants and sodium dodecyl sulfate show drastically different interactions. At pH 6 they show strong synergy, while at pH 11 they show antagonistic effects. Theoretical model for the adsorption of surfactant molecules at air-water interface have been initiated.

MATERIALS & METHODS

MATERIALS

Surfactants:

Several typical ionic and nonionic surfactants were selected for this study. Anionic sodium dodecyl sulfate (SDS) of greater than 99% purity purchased from Fluka chemicals and cationic dodecyl trimethyl ammonium bromide (DTAB) of greater than 99% purity purchased from TCI Chemicals, Japan was used as received. The nonionic ethoxylated alcohols C_nEO_m were purchased from Nikko Chemicals. Non-ionic sugar-based surfactant n-dodecyl- β -D-maltoside from Calbiochem and dodecyl polyglucoside from Henkel Corp. were also used as received. The structures of n-dodecyl- β -D-maltoside and dodecyl polyglucoside are shown in Figure 1. Dodecyl polyglucoside was an industrial sample with various headgroup configurations and glucose unit distributions, while n-dodecyl- β -D-maltoside was relatively pure (>95% purity by TLC) and served as a model compound for alkyl polyglucosides. These surfactants are listed in table I.

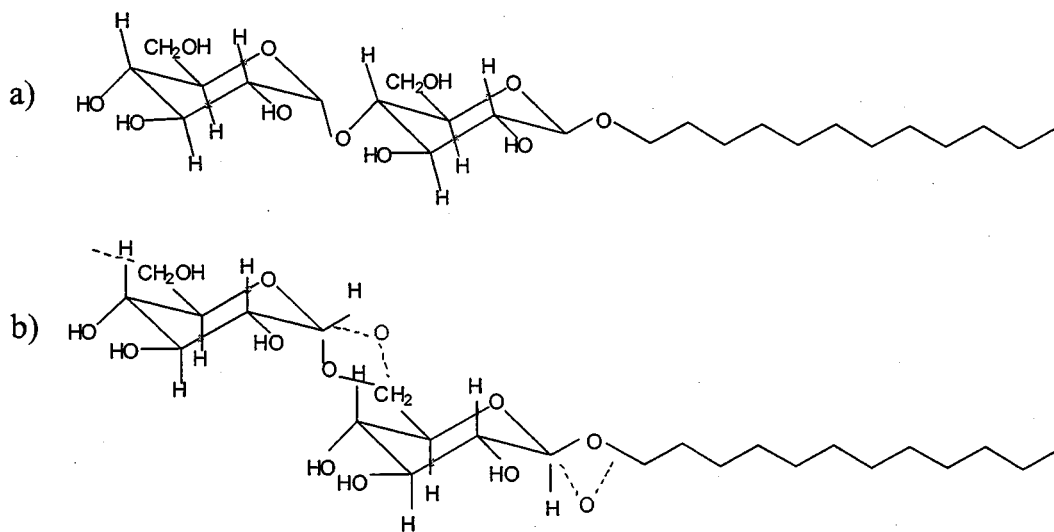


Figure 1. The Chemical Structures of a) n-dodecyl- β -D-maltoside, and b) dodecyl polyglucosides

Table 1. Surfactants used and their molecular structure

Surfactant	molecular structure
Sodium dodecyl sulfate	$C_{12}H_{23}SO_4Na$
Polyethoxylated alcohol	$C_nH_{2n+1}(CH_2CH_2O)_mH$
Dodecyltrimethylammonium bromide	$[CH_3(CH_2)_{11}N(CH_3)_3]Br$
n-dodecyl- β -D-maltoside	$C_{24}H_{46}O_{11}$
Dodecyl polyglucoside	$CH_3(CH_2)_{11}[C_6H_{10}O_5]_n$

Mineral Samples:

Solid substrates selected for this study were alumina and titania. Alumina AKP-50 obtained from Sumitomo Company had a mean diameter of 0.2 μ m and specific surface area of 10.8 m^2/g . The isoelectric point (iep) was 8.9. Titania from Alfa Products had a diameter of 2 μ m, specific surface area of 2.13 m^2/g and isoelectric point (iep) of 2. These solids were chosen because of their low solubility, and relatively surface homogeneity with considerable amount of information in the literature.

Other Chemicals:

Maltose was from Calbiochem and dimethyl sulfoxide from Sigma Chemical Co. Urea, $CaCl_2$, and HCl and NaOH of A.C.S. grade certified (purity > 99.9%) used for pH adjusting, were from Fisher Scientific Co. Water used in all experiments was triple distilled, with a specific conductivity of less than $1.5\mu\Omega^{-1}$ and was tested for absence of organics using surface tension measurements.

METHODS

Surface tension:

Surface tension of the surfactant solutions was measured using a Wilhelmy plate made of platinum.

Adsorption experiments:

Adsorption experiments were conducted in capped 20 ml vials. Solid samples of 0.4 gram were mixed with 10 ml of triple distilled water (TDW) for 2 hours at room temperature. The pH was adjusted as desired and then 10 ml of the surfactant solution was added and the equilibrated further for 16 hours. The samples were then centrifuged next for 30 minutes at 5000 rpm and about 10 ml of the supernatant was pipetted out for analysis.

Desorption:

After adsorption, desorption tests were conducted by removing part of the supernatant and adding water to make up for the volume of the supernatant removed. The total volume and thus solid-liquid ratio remained constant. Adsorption density was calculated from the change in concentration of the surfactant.

Analytical Techniques:

Sodium dodecyl sulfate (SDS) concentration was determined using a two-phase titration method¹. Sugar-based surfactant concentration after adsorption was determined by measuring the total organic carbon (TOC) in the sample using a Dohrmann Carbon Analyzer, or by colorimetric method through phenol-sulfuric acid reaction.² In surfactant mixtures, the total surfactant concentration was measured by TOC method, while the SDS concentration was measured by the two-phase titration and sugar-based

¹ Z. Li and M.J. Rosen, *Analytical Chemistry*, **53**, 1981, 1516.

² Dubois, M., Gilles, K. A., Hamilton, J. K., Rebers, P. A., Smith, F., "Colorimetric Method for Determination of Sugars and Related Substances", *Anal Chem*, **28**, 1956, 350

surfactant by the colorimetric method.

Electrokinetics:

Zeta potential of the samples was determined using a Pen Kem Laser Zee Meter. After surfactant adsorption, the sample was diluted with its own supernatant to make a dispersion of suitable solid concentration.

Calcium Ion Measurement:

The Ca^{2+} ion concentration was measured by an Orion Research Microprocessor Ionalyzer (model 901) using a calcium electrode (Orion Research).

FTIR Spectroscopy:

A Perkin Elmer Paragon 1000 PC FTIR spectrometer was used to record the IR spectra for the attenuated total reflectance(ATR). ATR was conducted in-situ for solid/liquid slurries in a nine-reflection prism cell (ZnSe, 45°) supplied by Harrick scientific Co.

RESULTS & DISCUSSION

I. Adsorption Mechanism of n-dodecyl- β -D-maltoside on Alumina

In our previous study, adsorption behavior of a sugar-based nonionic surfactant, n-dodecyl- β -D-maltoside, on various hydrophilic and hydrophobic solids has been examined. Interestingly, it was found that this surfactant adsorbs on alumina, hematite and titania, but markedly less on silica. This behavior is opposite to that of the nonionic ethoxylated surfactants, which adsorb on silica but not on alumina and hematite. This unique behavior of sugar-based surfactants, plus the environmental advantage of these biodegradable substance, enable them to be utilized in various applications such as flocculation/dispersion, wetting and enhanced oil recover. Since adsorption on silica and silicates are relevant to EOR systems, it is important to explore the reasons for the different adsorption behavior of these surfactants for efficient usage of them.

It is known that polysaccharide polymers such as dextrin and starch also adsorb on alumina and hematite but not on silica. This behavior is similar to that of n-dodecyl- β -D-maltoside. Since n-dodecyl- β -D-maltoside, as well as alkyl polyglucosides, has oligo-saccharide headgroups, the interactions between their headgroups and oxides could be similar to those between polysaccharide polymers and oxides. Hydrogen bonding has been proposed as the driving force for the adsorption of polysaccharides. However, some experimental evidence has been obtained suggesting also chemical interactions between polysaccharides and oxides. In this study, adsorption mechanism of n-dodecyl- β -D-maltoside was investigated systematically by combining adsorption and electrokinetic observations and spectroscopic analysis with theoretical considerations.

1. Adsorption/Desorption of n-dodecyl- β -D-maltoside on alumina

Adsorption isotherm of n-dodecyl- β -D-maltoside on alumina is shown in Figure 2 along with the

corresponding desorption isotherm. The isotherm shows a typical three stage adsorption with a very low adsorption at low concentrations, a sharp increase at concentrations close to the critical micelle concentration of the surfactant, and a plateau region at concentrations higher than CMC. It is to be noted that the isotherm has a very small slope in the low concentration range, indicating weak driving force for adsorption, since stronger interactions such as electrostatic interactions would result in a slope of 1 at low concentrations under constant ionic strength conditions. The S shape of the adsorption isotherm indicates strong interactions between the adsorbate species, in this case hydrophobic chains, and comparatively weaker interactions between the adsorbate and the adsorbent. The corresponding desorption isotherm shows that the adsorption process is reversible with no hysteresis under the tested conditions. This also suggests a lack of strong specific interactions such as chemisorption between this surfactant and the solid.

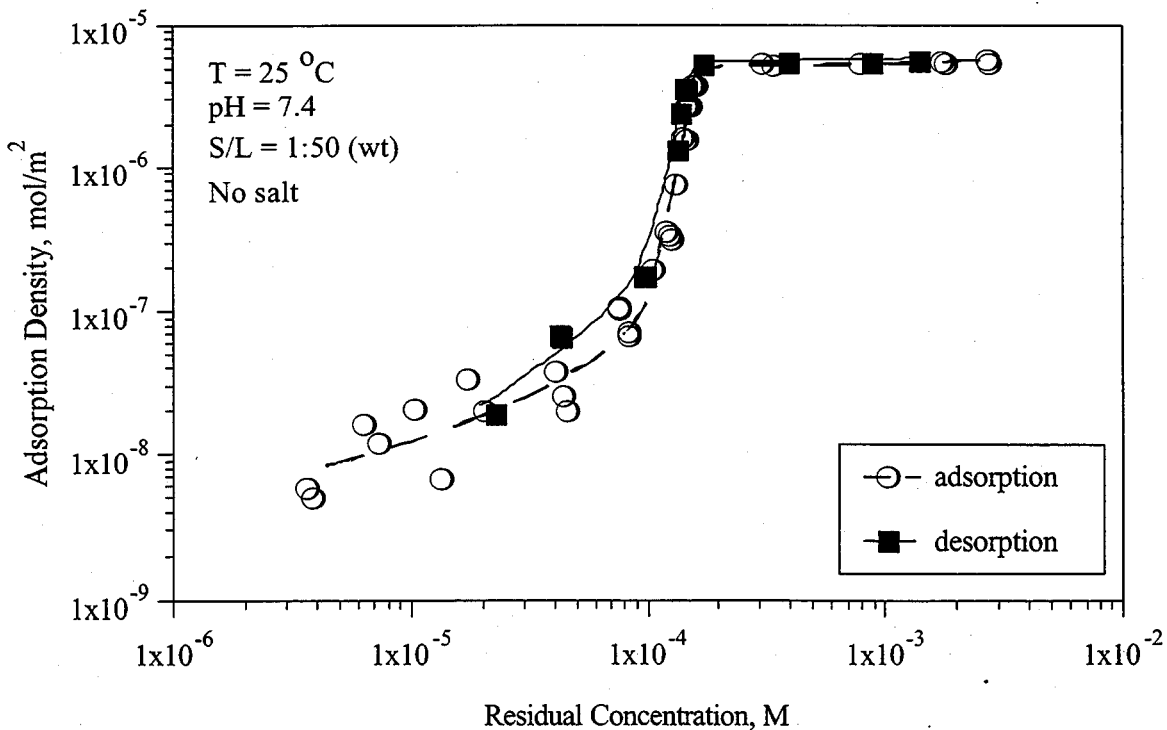


Figure 2. Adsorption and Desorption Isotherms of n-Dodecyl- β -D-Maltoside on Alumina

2. Effect of pH on the adsorption of n-dodecyl- β -D-maltoside on alumina

In order to check if the electrostatic interaction is the driving force for adsorption, the effect of pH on the adsorption of DM on alumina was carried out and the results obtained are shown in Figure 3. The isoelectric point of alumina is 8.9. The alumina is positively charged at pH 7.4 and negatively charged at pH 11. The surfactant adsorption is not affected by the change in pH, suggesting that surface charge of alumina does not govern the adsorption of n-dodecyl- β -D-maltoside under the tested conditions.

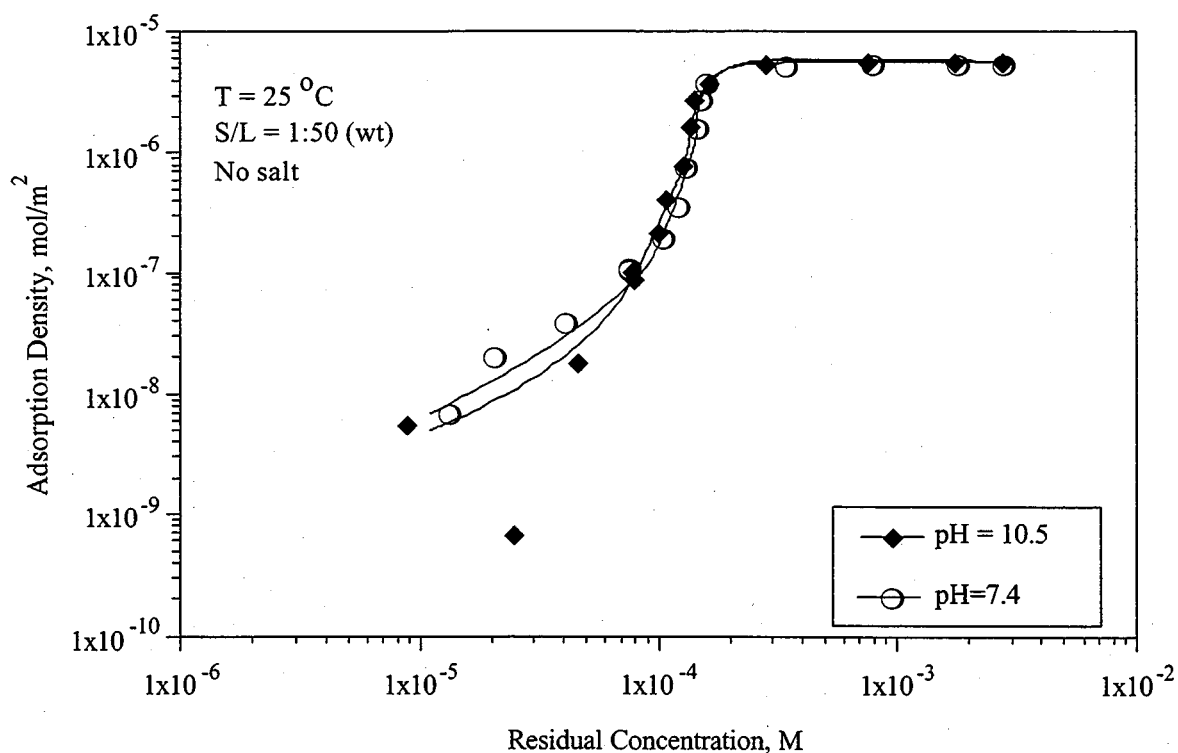


Figure 3. Effect of pH on the Adsorption of n-Dodecyl- β -D-Maltoside on Alumina

3. Zeta-potential of alumina after n-dodecyl- β -D-maltoside adsorption

In order to further examine the role of electrostatic interactions, electrokinetic measurements were made on alumina after n-dodecyl- β -D-maltoside adsorption and the results are shown in

Figure 4. The zeta-potential of alumina changed only slightly by the adsorption of DM surfactant. This small decrease of zeta-potential in the case of alumina is proposed to be due to the masking of the solid surface by the adsorbed surfactant species. These results are in accord with the non-ionic nature of the n-dodecyl- β -D-maltoside and eliminate the possibility of any electrostatic interaction between the solid and the surfactant.

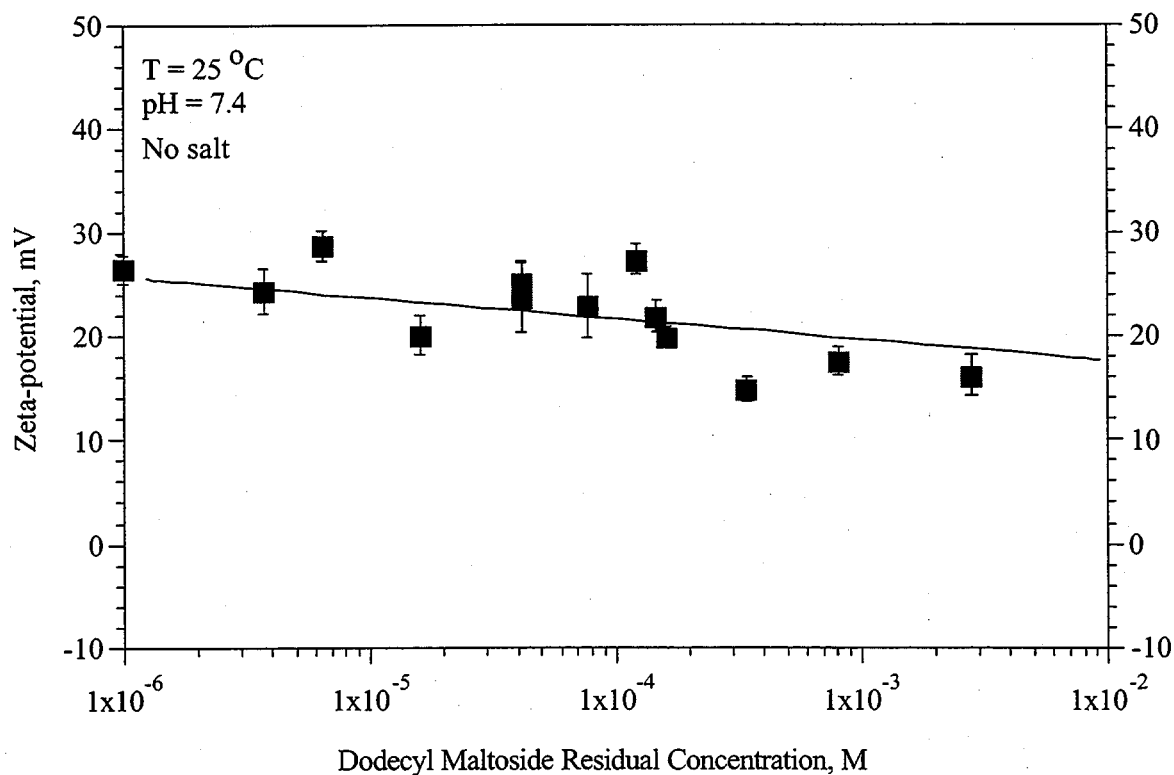


Figure 4. Zeta-potential of Alumina after n-Dodecyl- β -D-Maltoside Adsorption at Neutral pH

4. Interaction between calcium ion and n-dodecyl- β -D-maltoside

Multivalent metal cations such as calcium and aluminum ion are known to interfere with the performance of some surfactants by precipitation or complexation. No such interactions have been found for n-dodecyl- β -D-maltoside in solution by surface tension studies. To further explore the possibilities of

such interactions, the concentration change of calcium ion has been measured in the presence of n-dodecyl- β -D-maltoside using conductivity technique.

Two DM concentrations were chosen such that one is with surfactant micelles in solution while the other is without. The results illustrated in Figure 5 show the calcium ion conductivities in water, 0.1 mM and 0.5 mM DM solutions to be identical. It can therefore be concluded that there is no interaction between calcium ion and n-dodecyl- β -D-maltoside. Implications of the absence of calcium sensitivity to EOR is very important.

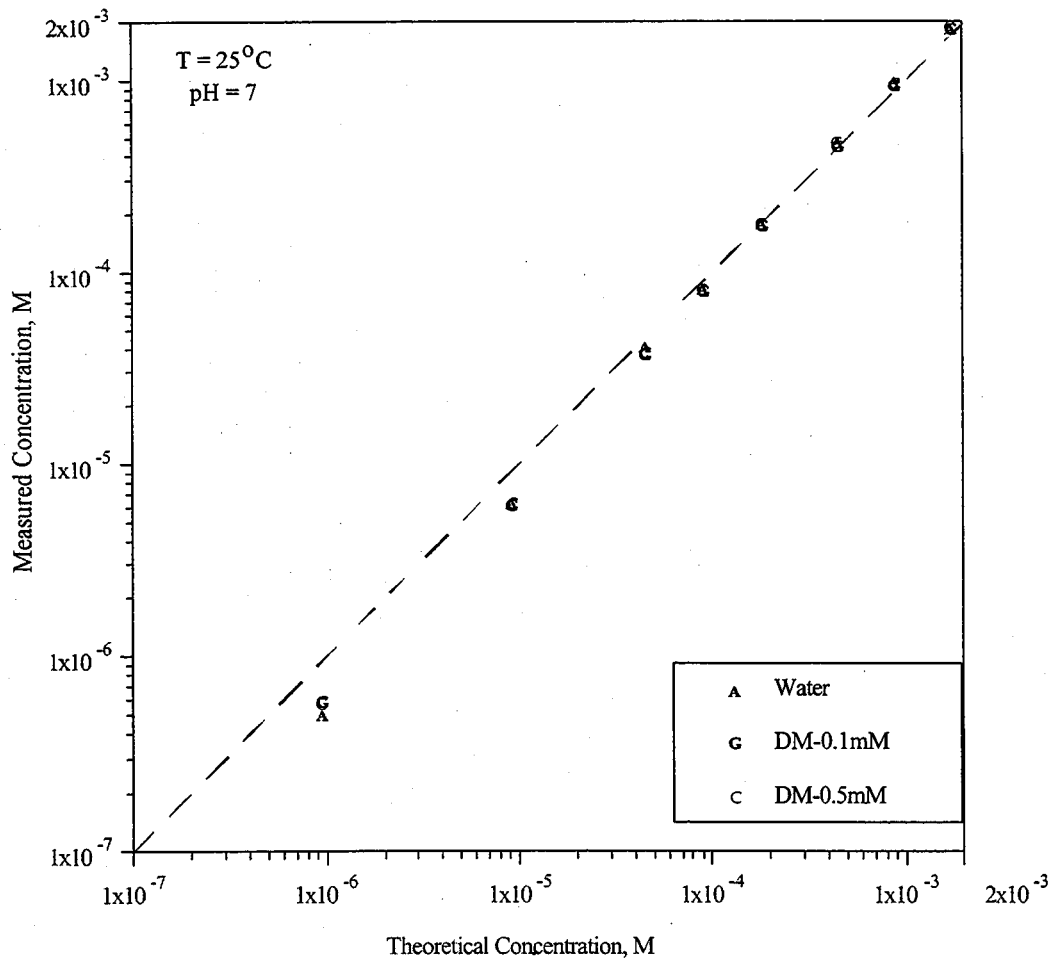


Figure 5. Effect of n-Dodecyl- β -D-Maltoside on the Calcium Conductivity

5. Adsorption of maltose on alumina

Since the adsorption of n-dodecyl- β -D-maltoside on alumina is considered to be first due to the interactions between surfactant maltose headgroup, and surface species of alumina, the adsorption of maltose on alumina was also investigated. The adsorption isotherm of maltose is shown in Figure 6 along with that for n-dodecyl- β -D-maltoside. There is only a small amount of maltose adsorbed on alumina and there is no sharp rise in adsorption, suggesting that there exists only weak interaction between maltose and alumina. The sharp rise in adsorption density in the case of dodecyl maltoside surfactant at higher concentrations is due to the hydrophobic interactions between the surfactant chains. This can be concluded by noting the different shapes of the adsorption isotherms for maltose and n-dodecyl- β -D-maltoside.

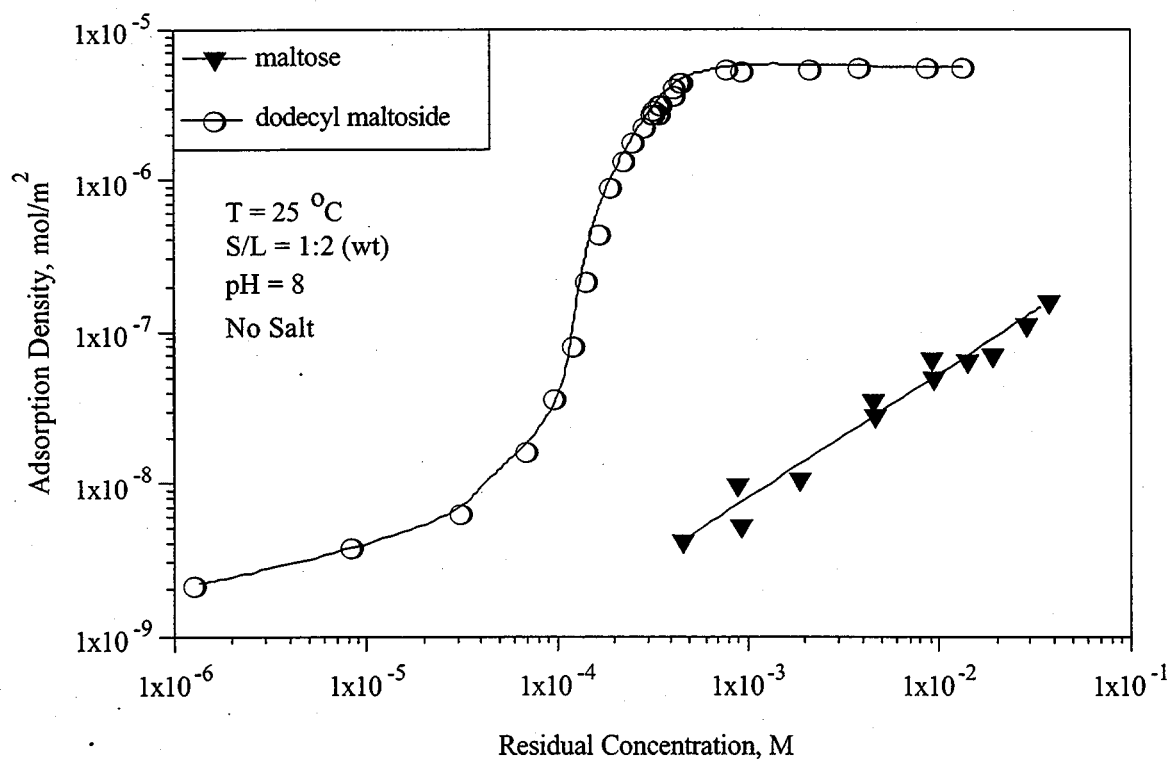


Figure 6. Adsorption of Maltose on Alumina Compared with that of n-Dodecyl- β -D-Maltoside

6. Effect of temperature on adsorption of *n*-dodecyl- β -D-maltoside on alumina

Adsorption of nonionic surfactants is usually sensitive to temperature. For ethoxylated surfactants, increase in temperature usually causes an increase in the adsorption density due to their dehydration at elevated temperatures. To investigate this aspect, the effect of temperature on the adsorption of *n*-dodecyl- β -D-maltoside on alumina is tested and results are shown on Figure 7. Temperature has almost no effect on the adsorption of *n*-dodecyl- β -D-maltoside. Also, the maximum adsorption density is not affected by the temperature change. The shift in inflection point (between sharp-rising region and plateau region) is mostly due to the increase in critical micelle concentration of the surfactant upon elevating the temperature. Since chemical reaction rate is a function of temperature, the negligible dependence of adsorption on temperature in this case suggests that there is no chemical interaction between the surfactant and the solid.

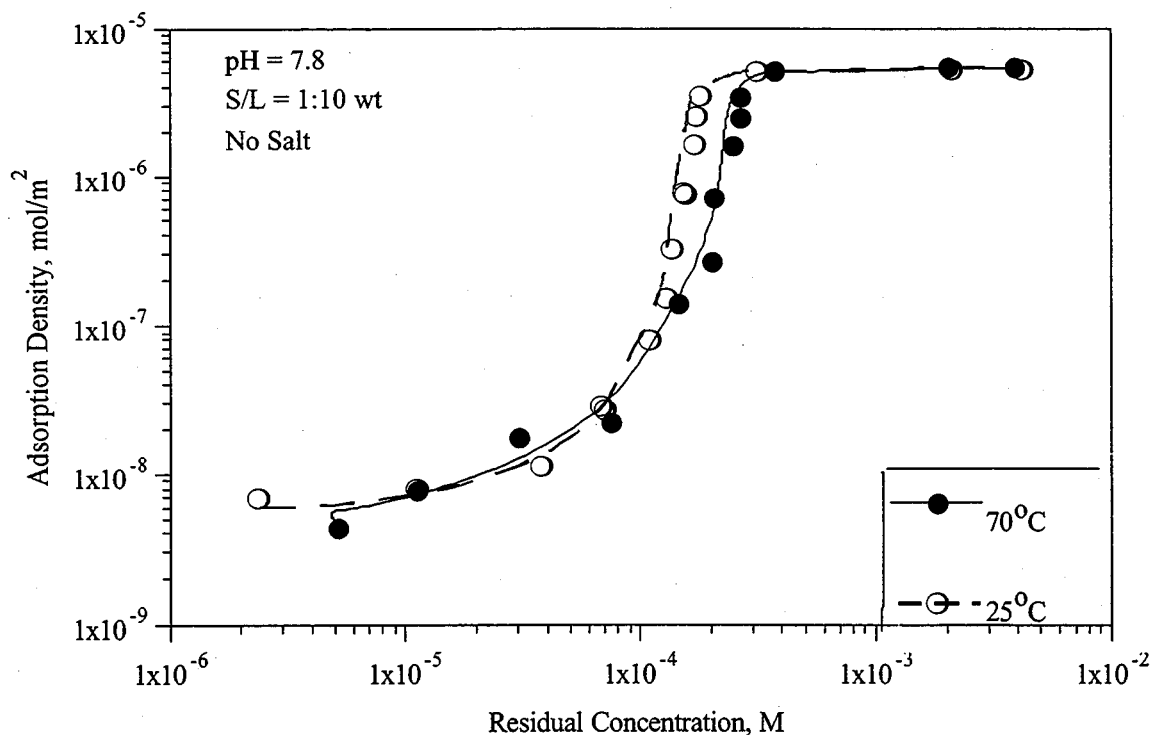


Figure 7. Effect of Temperature on the Adsorption of *n*-Dodecyl- β -D-Maltoside on Alumina

7. Adsorption/desorption of *n*-dodecyl- β -D-maltoside on alumina in urea and DMSO solutions

It is proposed that hydrogen bonding is the most possible driving force for the adsorption of *n*-dodecyl- β -D-maltoside on alumina. To test this hypothesis, adsorption in various solvents were carried out. Urea and dimethyl sulfoxide(DMSO) are strong hydrogen bonding acceptors. They can be expected to affect the hydrogen bonding between the solid substrate and the surfactant in solution by preferential formation of hydrogen bonds between themselves and with either the solid or the surfactant. The presence of urea or DMSO should affect the adsorption of *n*-dodecyl- β -D-maltoside on alumina, if hydrogen bonding is the driving force for the adsorption.

Adsorption and desorption isotherms of *n*-dodecyl- β -D-maltoside on alumina in urea and DMSO solutions are shown in Figures 8 and 9. The results show that adsorption density is affected markedly by both urea and DMSO. In urea solution, the maximum adsorption is lower and the inflection points of the isotherms are shifted to higher concentrations. Urea is known to affect the solvent properties. The DMSO

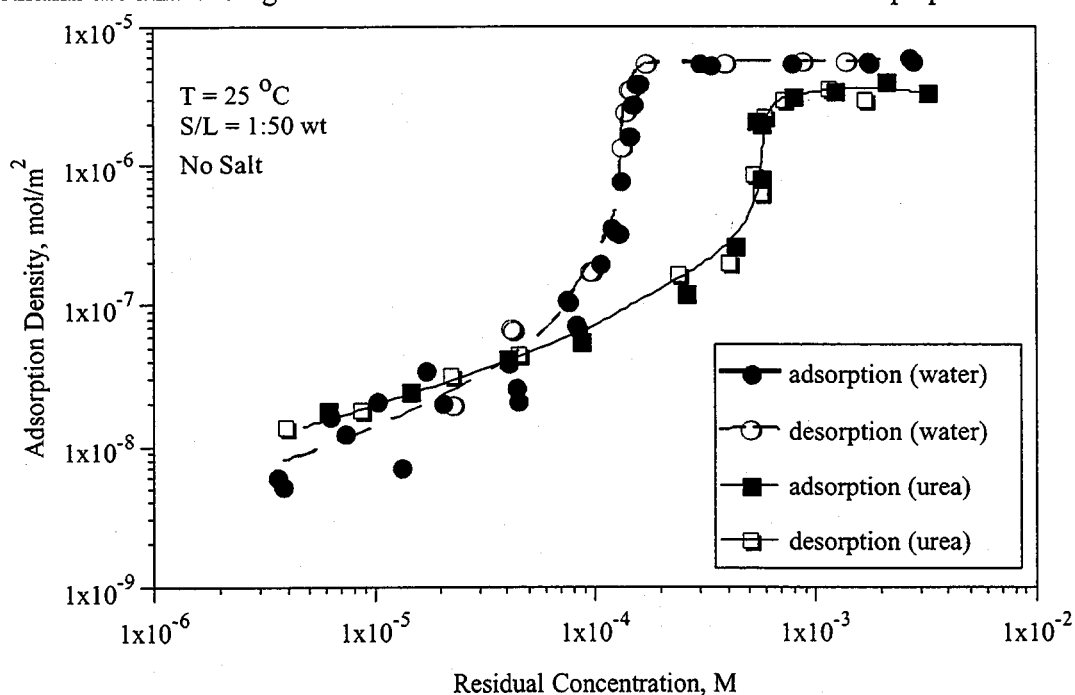


Figure 8. Adsorption and Desorption of *n*-Dodecyl- β -D-Maltoside in the Presence of 5M Urea

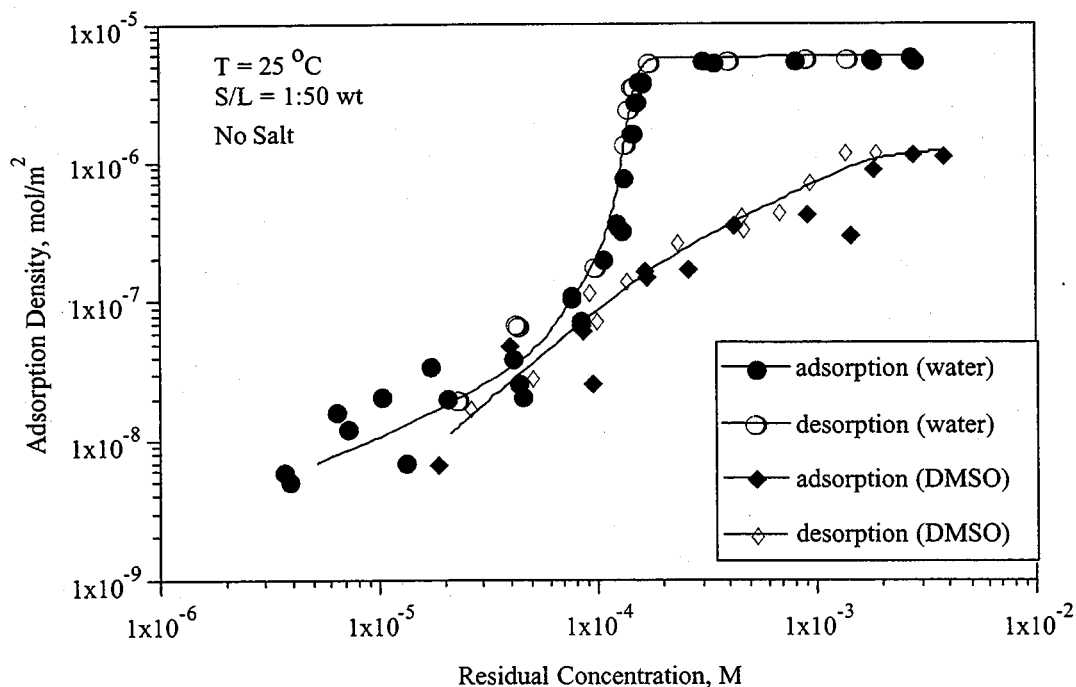


Figure 9. Adsorption and Desorption of n-Dodecyl- β -D-Maltoside in the Presence of 85% DMSO

not only decreased the adsorption density, but also yielded a very different isotherm shape. There is no clear inflection point on the isotherm in the 85% DMSO solution. These results suggest that hydrogen bonds between solid and surfactant are weakened in the presence of urea and DMSO. The different shapes of adsorption and desorption isotherms of DM on alumina in the 85% DMSO solution can be explained by the absence of DM aggregation at the solid/liquid interface. The sharp rise in the adsorption isotherm is obtained only when solloids (surface aggregates, hemimicelles) form.

8. Characterization of N-Dodecyl- β -D-Maltoside/Alumina Interactions by FTIR Spectroscopy

FTIR spectroscopy can give direct evidence for certain chemical interactions between surfactants and solids. Attenuated total reflectance (ATR) technique was used here to probe in-situ interactions of the

surfactant with the solid. The ATR spectra of n-dodecyl- β -D-maltoside in solution and adsorbed on alumina in the region 4000-400 cm^{-1} are shown in Figure 10A. The spectrum of adsorbed n-dodecyl- β -D-maltoside on surfaces was obtained by subtracting the spectrum of alumina slurry from that of alumina/surfactant system. As water was used for the background scan, the strong peak around 1640 cm^{-1} is attributed to the H-O-H bending of the water molecules. Strong absorption by water and the solid also occurs in the 4000-3000 cm^{-1} and 800-400 cm^{-1} regions.

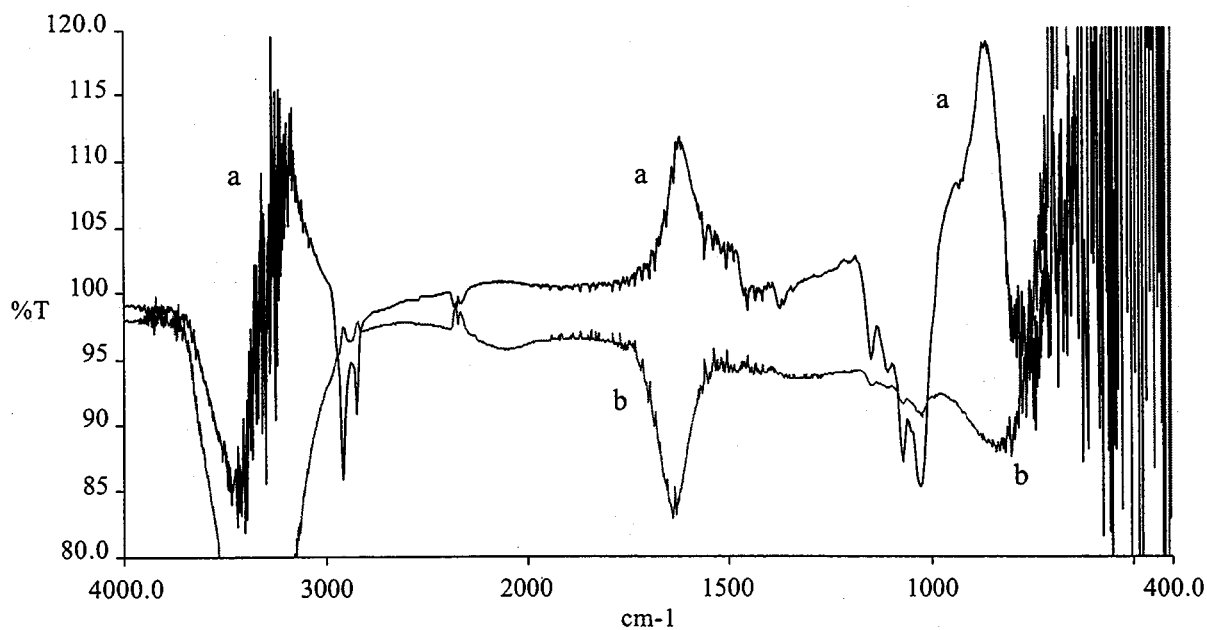


Figure 10. A) 4000-400 cm^{-1} ATR Spectrum of DM Adsorbed on Alumina with Alumina Subtracted(a), Compared to the Spectrum of DM in Solution (b) (T : Transmittance)

The 1300-700 cm^{-1} range is very infrared active for the polysaccharides. Spectra of the adsorbed surfactant and the surfactant in solution in the region 1200-800 cm^{-1} are shown in Figure 10b (enlarged from Figure 10a). In the spectrum of the adsorbed surfactant, the intense bands at 1149, 1075 and 1030 cm^{-1} are characteristic of various -C-OH stretchings of the glucose and the peak at 859 cm^{-1} is for the ring vibration. The spectrum of the surfactant in solution has no strong absorption bands. The bands at 1075,

1027, 836, 822, 819 and 807 cm^{-1} shift very slightly upon adsorption of the surfactant, indicating no chemical interaction between the surfactant and alumina.

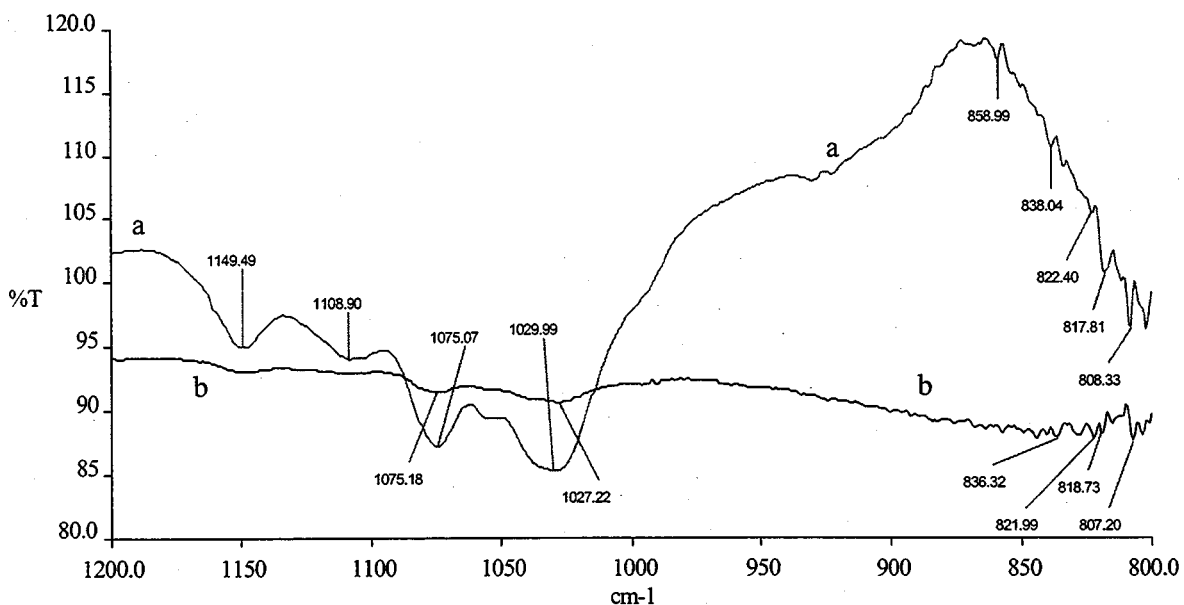


Figure 10. B) 1200-800 cm^{-1} ATR Spectrum of DM Adsorbed on Alumina with Alumina Subtracted(a), Compared to the Spectrum of DM in Solution (b)

To further explore the adsorption of n-dodecyl- β -D-maltoside on alumina, the spectrum of maltose/alumina system was also studied since maltose is the functional group on the former. The ATR spectra obtained for maltose in solution and at solid/liquid interface show that the peaks of the maltose adsorbed on solid surfaces are similar to those of maltose itself, indicating that there is no chemical interaction between maltose and alumina as well (Figure 11).

The spectra of n-dodecyl- β -D-maltoside and maltose in solution and those at the solid/liquid interface show no significant band shift due to the adsorption over the region studied. These results further suggest that the adsorption of n-dodecyl- β -D-maltoside on alumina is not due to specific interactions between the DM surfactant and the solid.

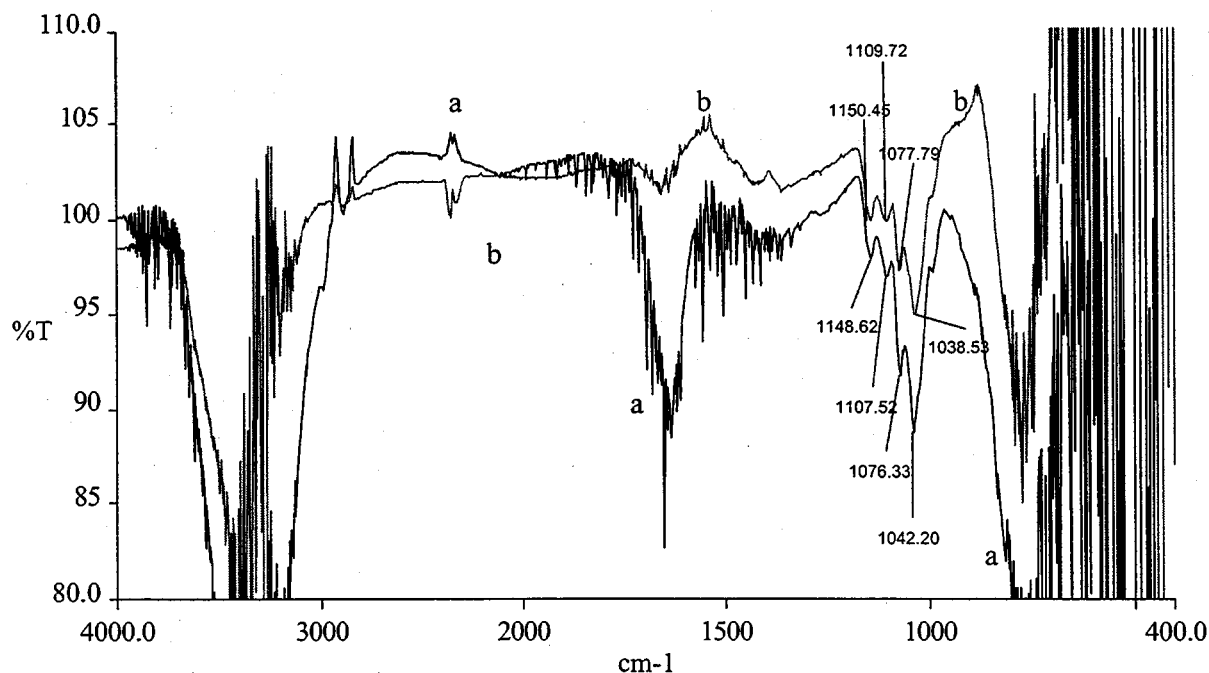


Figure 11. ATR Spectrum of Maltose Adsorbed on Alumina with Alumina Subtracted(a), Compared to the Spectrum of Maltose in Solution (b)

It is therefore proposed that hydrogen bonding between hydroxyl groups on the surfactant and alumina surface hydroxyl species is the driving force for the adsorption of n-dodecyl- β -D-maltoside on it. Experimental evidence for hydrogen bonds formed between surfactant hydroxyl groups and solid surface hydroxyl groups in aqueous solution is rather difficult to obtain, since water molecules are capable of hydrogen bonding extensively with each other and with hydroxyl groups of the solids and the surfactants. However, disruption of the adsorption by hydrogen bond breaker has been observed. By elimination of other possibilities such as electrostatic interactions and chemical interactions, hydrogen bonding is proposed to be the most possible driving force for the adsorption of n-dodecyl- β -D-maltoside on alumina. These results suggest that potential loss of sugar-based surfactants by adsorption on oil field rocks is likely to be minimal. This and the insensitivity to calcium may be two significant advantages for using sugar-based surfactants in enhanced oil recovery (EOR).

II. Surface Tension of Sugar-based Surfactants with Anionic Surfactant

To better understand the surfactant interactions at solid/liquid interface relevant to the enhanced oil recovery process, it is necessary to have also a knowledge of their solution behavior. It was also an aim to investigate the properties of surfactant mixtures in solution by studying their surface tension behavior.

The interactions of sugar-based dodecyl polyglucoside (C12-APG) and n-dodecyl- β -D-maltoside (DM) with a typical anionic surfactant, sodium dodecylsulfate (SDS), was studied with and without a supporting electrolyte in the solution. As they all have the same hydrophobic chain length, any deviation from ideality can be ascribed to dissimilarity in the hydrophilic headgroups.

1. Surface tension of n-dodecyl- β -D-maltoside and sodium dodecylsulfate mixtures

Surface tension data for DM, SDS, and DM/SDS 3:1, 1:1, and 1:3 mixtures, with and without salt, are shown in Figures 12 and 13 as a function of the total concentration. The relevant data such as the critical micelles concentrations, the mole fraction of DM in the mixed micelles, and the interaction parameters of the mixtures are listed in Tables 2 and 3. The mole fractions and interaction parameters are calculated using the regular solution theory.

From Figures 12 and 13 as well as Tables 2 and 3, it can be concluded that in the surfactant mixture, dodecyl maltoside has the predominant role in mixed micellization at various mixture ratios. It is also the dominant component in the micellar phase. In surfactant mixtures, the component that has a lower cmc usually will be presented in a higher percentage in micelles and at the air-water interface because of its higher surface activity. These results are in accord with the fact that DM is much more surface active than sodium dodecylsulfate.

Table 2 Results of Surface Tension Data Analysis for DM/SDS Mixtures Without Salt at 25°C

DM : SDS	100 : 0	75: 25	50 : 50	25 : 75	0 : 100
cmc (M)	0.00018	0.000196	0.000255	0.000438	0.008
DM mole fraction in micelle		0.867	0.801	0.731	
interaction parameter β		-4.00	-3.77	-3.25	
average β	-3.67				

Table 3 Results of Surface Tension Data Analysis for DM/SDS Mixtures With Salt at 25°C

DM : SDS	100 : 0	75: 25	50 : 50	25 : 75	0 : 100
cmc (M)	0.000169	0.000179	0.000227	0.000349	0.00267
DM mole fraction in micelle		0.833	0.774	0.719	
interaction parameter β		-1.70	-2.78	-4.19	
average β	-2.89				

The average interaction parameter β is -3.67 for the system without salt and -2.89 for system with, indicating strong interaction between DM and SDS. This β value is typical of nonionic-ionic mixed surfactant systems. The synergy comes from two factors. First, the mixing of an ionic surfactant with a nonionic surfactant will cause a decrease in the surface charge density of the micelles, so that a mixed micelle of ionic and nonionic surfactants is more stable than a micelle containing only the ionic surfactant. Second, these different surfactant headgroups at the micellar surface can reduce the steric repulsion. Both factors favor micellization.

The presence of salt is found to reduce the synergy between the surfactants. In 0.03M NaCl the interaction parameter of DM/SDS is reduced from -3.67 to -2.89. This is mainly due to charge neutralization by the sodium counterions.

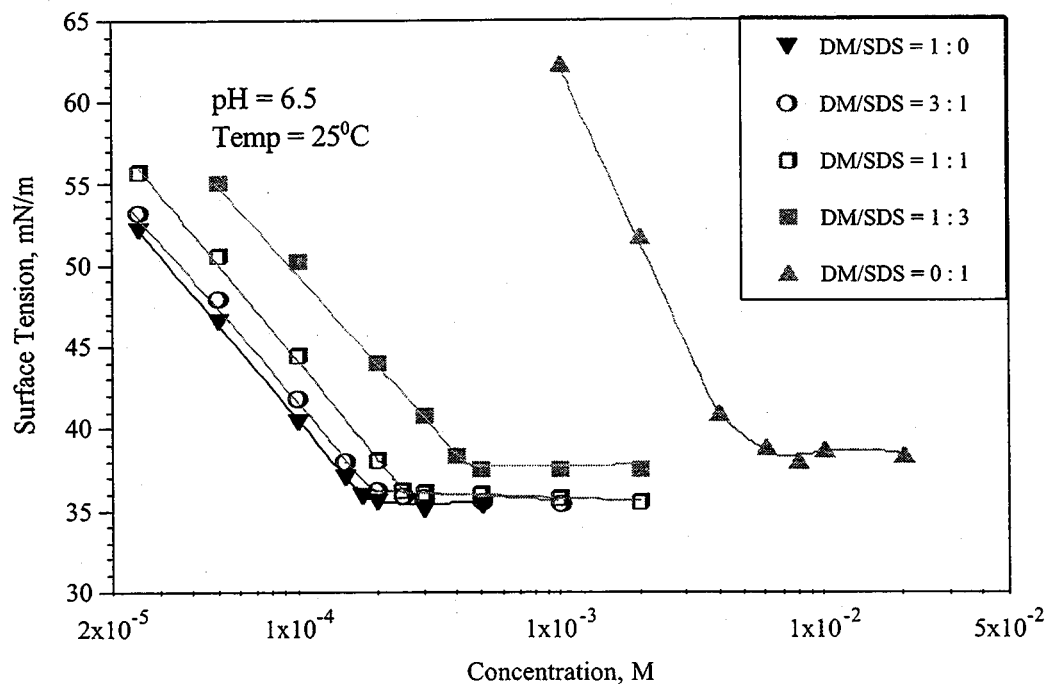


Figure 12 Surface Tension vs. Concentration of DM/SDS Mixed Surfactant System Without Salt

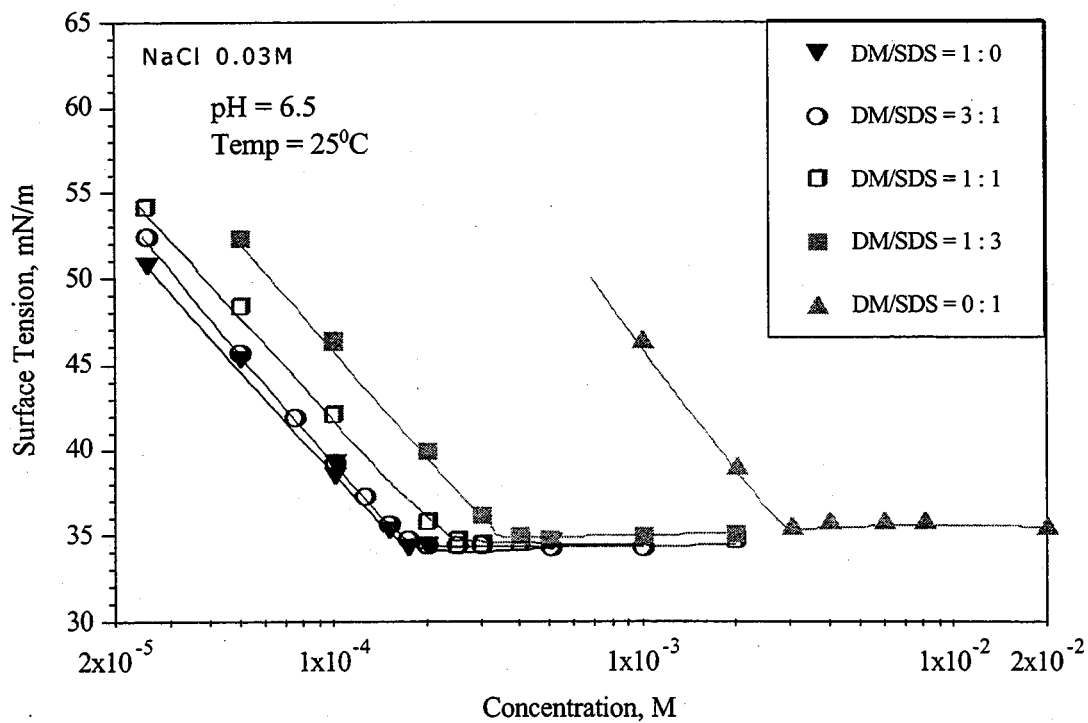


Figure 13 Surface Tension vs. Concentration of DM/SDS Mixed Surfactant System With Salt

2. Surface tension of dodecyl polyglucoside and sodium dodecylsulfate mixtures

To correlate the laboratory dodecyl maltoside sample with industrial alkyl polyglucoside samples, dodecyl polyglucoside (C_{12} -APG)/SDS system was studied next. Surface tension data obtained for the dodecyl polyglucoside mixture with the anionic SDS is plotted in Figure 14. Again, it is seen that APG is dominant in the APG/SDS mixtures. The interaction parameter for this system is -3.20 , suggesting strong synergy. Similarity in interactions between DM/SDS and APG/SDS also implies that commercial polyglucosides are similar to pure laboratory samples with respect to synergistic interactions with the anionic surfactant, suggesting that the pure alkyl polyglucosides may be used for studying interactions of sugar-based surfactants in general

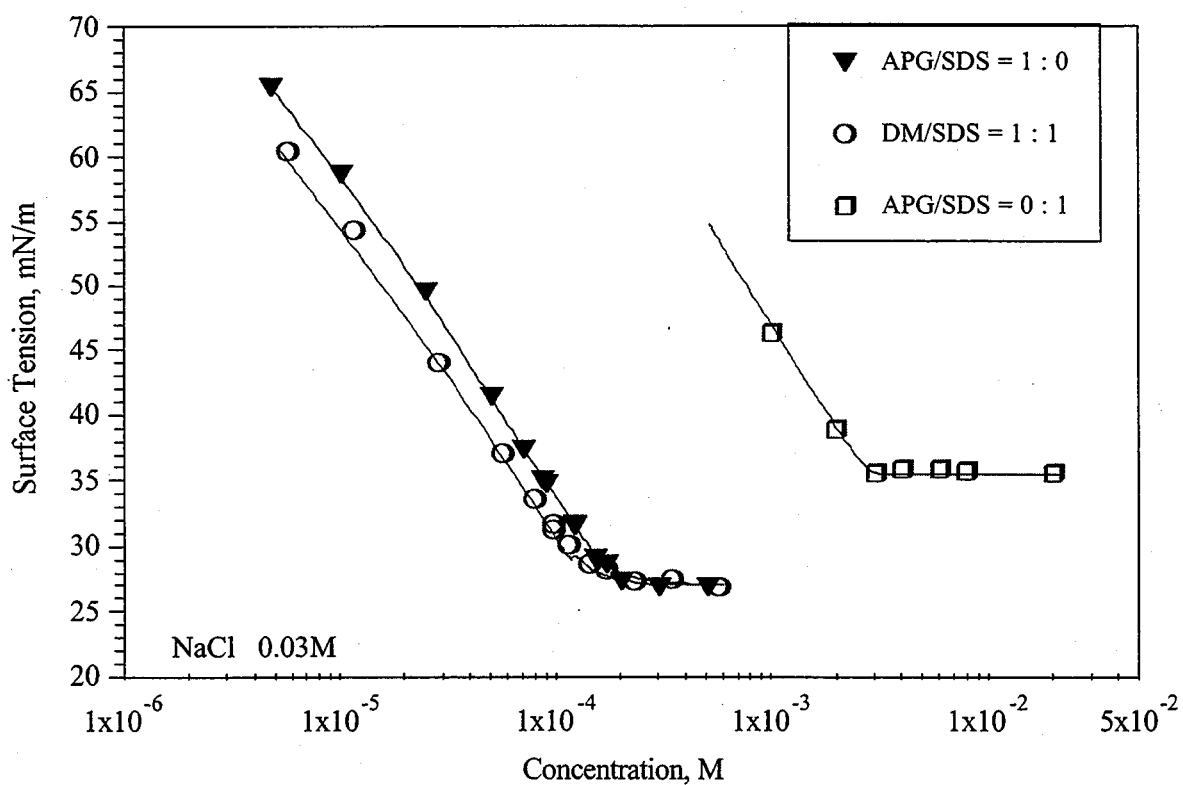


Figure 14 The Surface Tension vs. Concentration of C_{12} APG/SDS Mixed Surfactant System With Salt

III. Adsorption of Sugar-based Surfactants along with Anionic Surfactant at pH 6

Adsorption of nonionic-anionic mixtures of dodecyl polyglucosides (C12-APG)/sodium dodecyl sulfate (SDS), as well as n-dodecyl- β -D-maltoside (DM)/ sodium dodecyl sulfate (SDS), on alumina at pH 6 was studied. This is as part of our effort to understand the effect of pH change in these mixtures. The study of the adsorption behavior under different pH conditions offers an opportunity to observe possible synergism or antagonism between the two surfactants, and to compare the commercial sugar-based surfactants with laboratory counterparts.

1. Adsorption of dodecyl polyglucoside/sodium dodecylsulfate and n-dodecyl- β -D-maltoside/sodium dodecylsulfate 1:1 mixtures

The adsorption isotherms of dodecyl polyglucoside/sodium dodecyl sulfate 1:1 mixture and n-dodecyl- β -D-maltoside/sodium dodecyl sulfate 1:1 mixture on alumina at pH 6 are shown in Figures 15 and 16, together with those of dodecyl polyglucoside, dodecyl- β -D-maltoside and sodium dodecyl sulfate alone. The adsorption of the mixtures is higher than either of the components in the sharp rising part of the isotherm, showing strong synergy between the sugar-based surfactants and sodium dodecyl sulfate. This is the region where hydrophobic chain-chain interaction dominates the adsorption process, with the surface not yet saturated with the surfactant. At lower concentrations, SDS adsorbs more than APG or DM. In this region, adsorption takes place mainly due to electrostatic attraction between the negatively charged surfactant and positively charged alumina. Some adsorption of the sugar-based surfactant is evidently due to hydrogen bonding. At higher concentrations, the adsorbed SDS forms mixed aggregates with APG/DM through hydrophobic chain-chain interactions and promotes the APG/DM adsorption. The low critical micellar concentration of APG/DM causes the aggregates to form at lower concentrations and this promotes total adsorption as well. In the plateau region, the adsorption density of the mixture is slightly less

than that of SDS. As the surface is usually saturated with surfactants under these conditions, this can be attributed to the larger head group of the sugar-based surfactant.

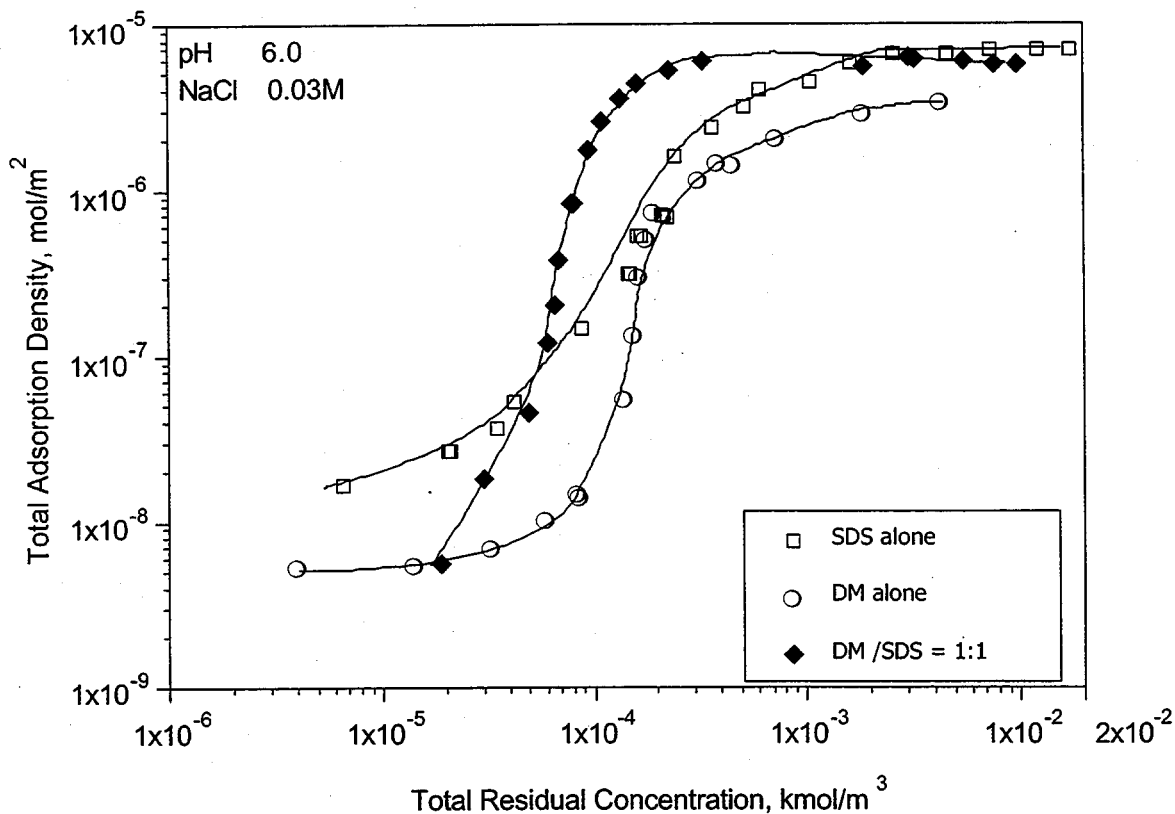


Figure 15. Adsorption of DM, SDS and DM/SDS 1:1 Mixture on Alumina

Adsorption behavior of dodecyl polyglucoside/sodium dodecyl sulfate is comparable to that of n-dodecyl- β -D-maltoside/sodium dodecyl sulfate but with much less synergy. The head group of the dodecyl polyglucoside in this study has an average DP (degree of polymerization) of 1.8. This is very close to that of dodecyl maltoside (DP = 2).

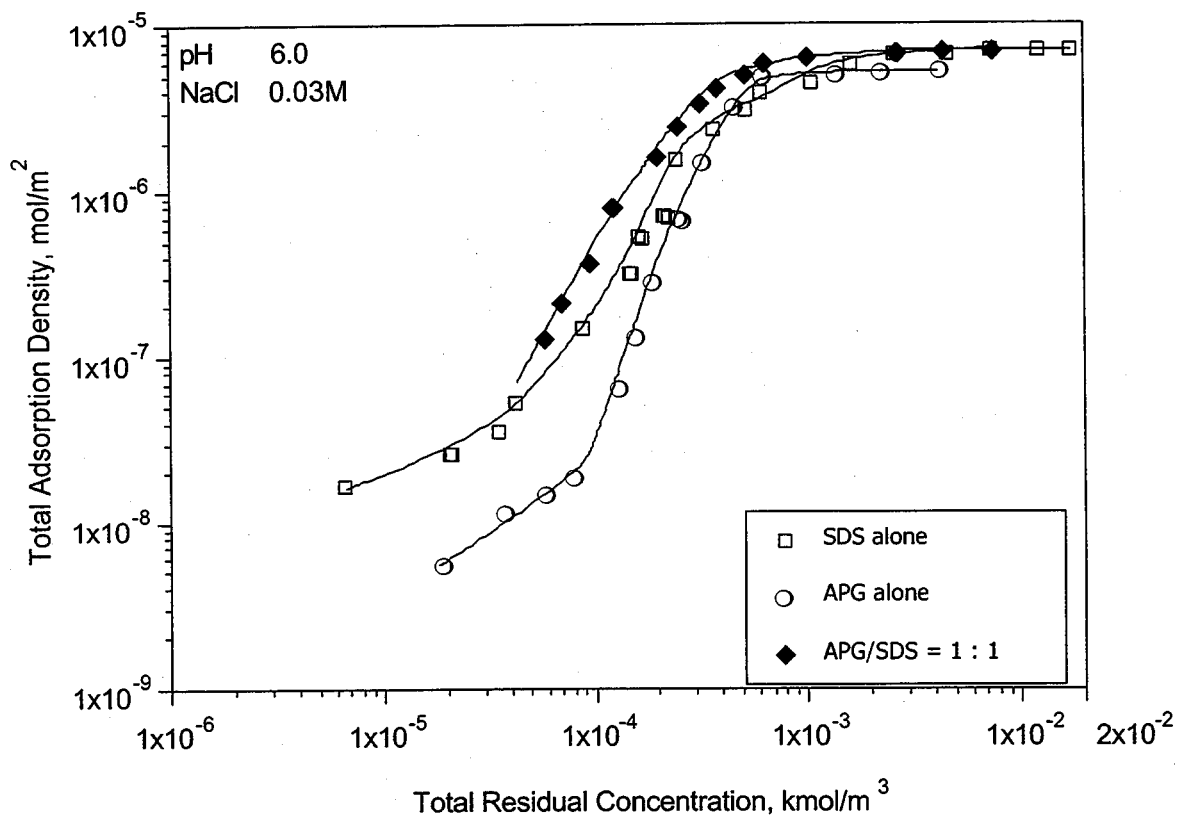


Figure 16. Adsorption of C_{12} -APG, SDS and C_{12} -APG/SDS 1:1 Mixture on Alumina

2. Adsorption of *n*-dodecyl- β -D-maltoside/sodium dodecylsulfate 3:1 and 1:3 mixtures

Experiments were also done for other mixing ratios of DM/SDS. The adsorption of DM, SDS and their 3:1, 1:1 and 1:3 mixtures are illustrated in Figure 17. All mixtures show synergistic effects in the rising part of the isotherms. It is interesting that DM/SDS 1:1 mixture shows the strongest synergy, suggesting that the synergistic action is stoichiometric due to possible 1:1 complex formation or better packing.

The adsorption densities of sodium dodecyl sulfate alone and from the DM/SDS mixtures on alumina are plotted in Figure 18 as a function of residual SDS concentration. Clearly the adsorption of SDS from the mixtures is higher than that of SDS from its single component solutions in the

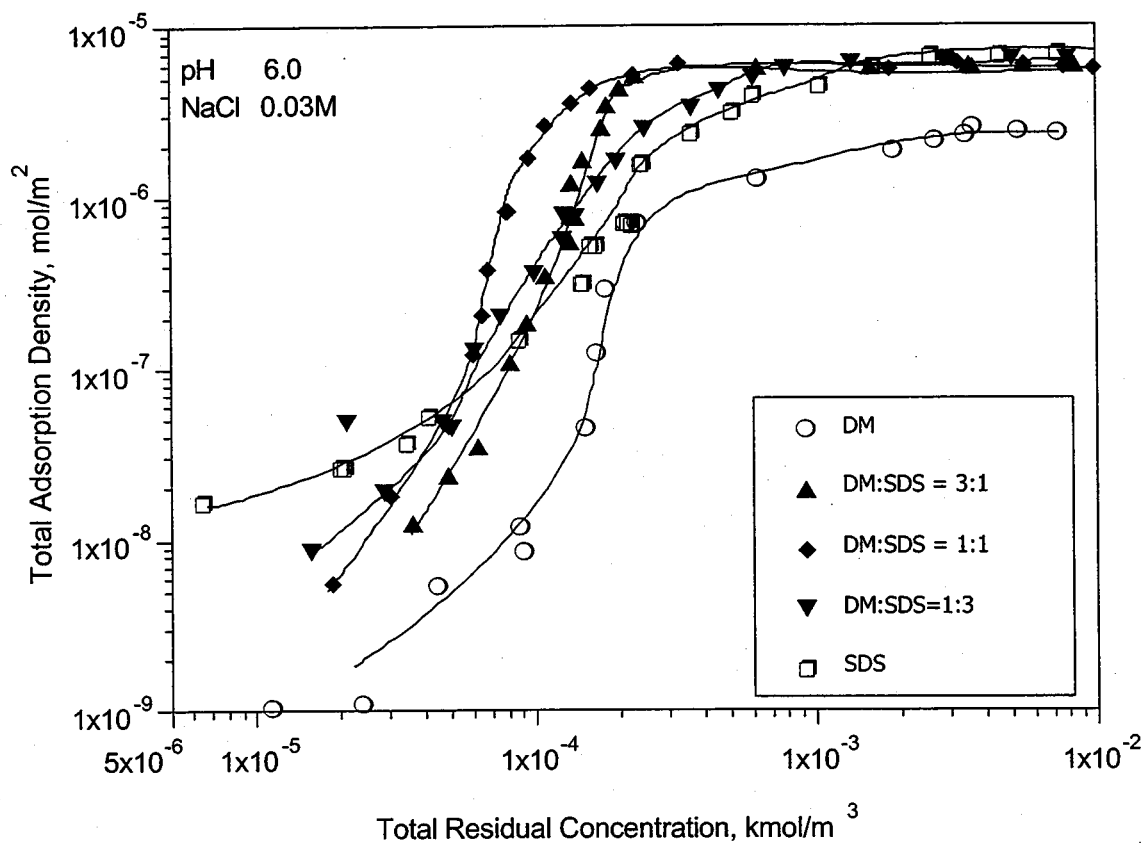


Figure 17. Adsorption of DM, SDS and their 3:1, 1:1 and 1:3 Mixtures on Alumina

sharp rising part of the isotherm. The more DM in the system (the higher the DM/SDS ratio), higher is the adsorption density at give concentrations, suggesting that the presence of DM promotes SDS adsorption. As mentioned above, in the plateau region, the surface is saturated with surfactant, and under these conditions the adsorption of SDS is lower than that when it is present alone due to competition from DM in the system. The higher the DM in the mixing ratio, the lower the adsorption of SDS, suggesting that more SDS is replaced by DM at the solid/liquid interface.

Similar data for DM adsorption alone from the DM/SDS mixtures and that from DM is given in Figure 19. It can be seen that the adsorption of DM is enhanced by the SDS in this case in the entire concentration range. Interestingly, more the SDS in the system, higher is the adsorption of DM in the rising part.

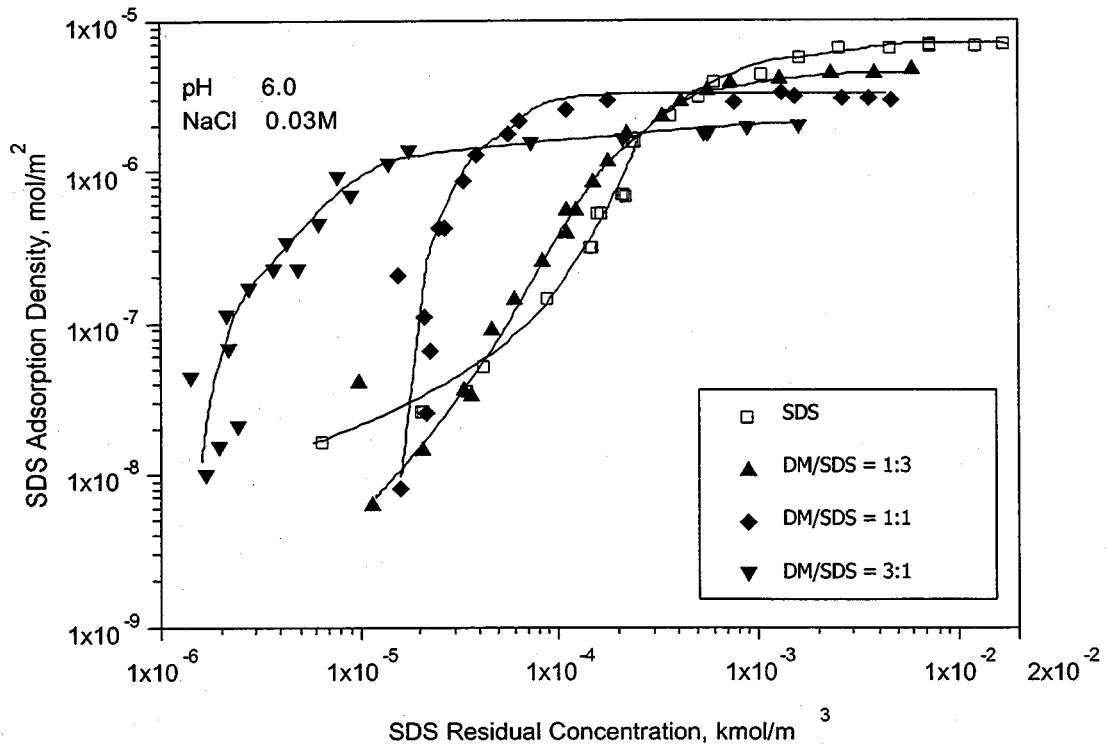


Figure 18. Adsorption of SDS on Alumina: Adsorption for SDS alone and from DM/SDS 3:1, 1:1 and 1:3 Mixtures

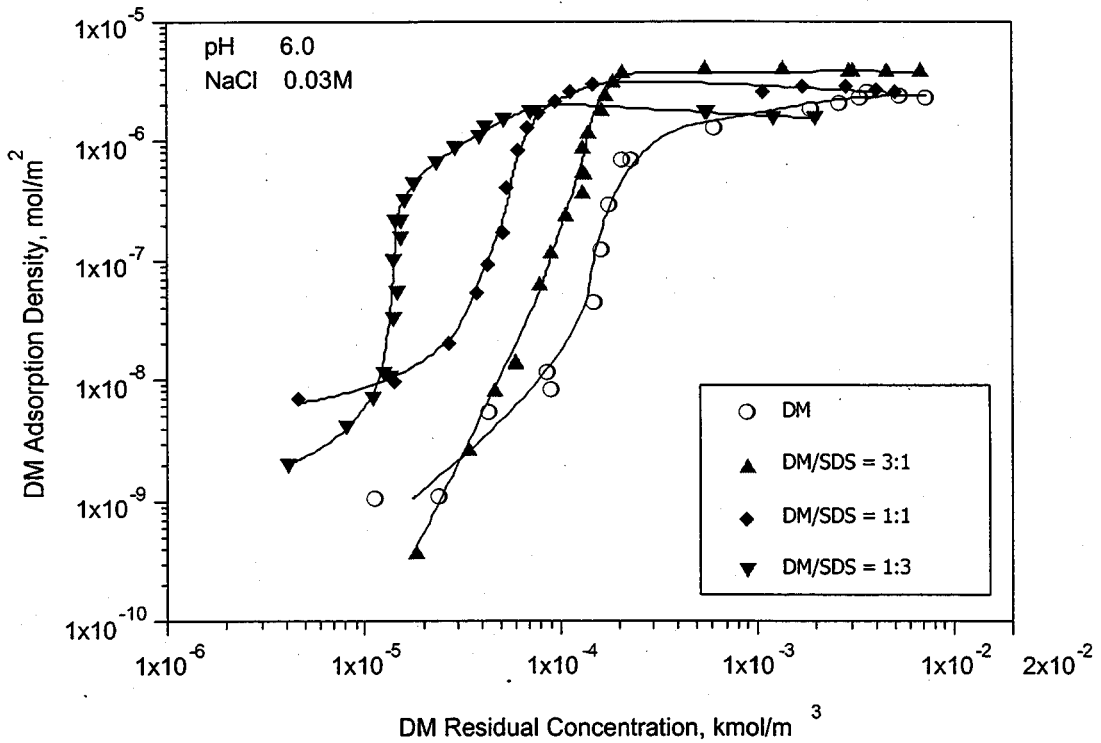


Figure 19. Adsorption of DM on Alumina: Adsorption for DM alone and from DM/SDS 3:1, 1:1, 1:3 Mixtures

Composition of the adsorbed layer will determine to a larger extent the interfacial behavior of the particles and hence it is plotted in Figure 20 as a function of the residual concentration of the surfactant in the mixture. In the case of DM/SDS 1:1 and 1:3 mixtures, the ratio at the S/L interface is very close to the bulk mixing ratio. However, for the 3:1 mixture, the DM/SDS ratio is small at low concentrations and reaches a maximum at the on-set of the adsorption plateau and then decreases again. In the entire concentration range tested, the DM/SDS ratio is smaller than 3, the total mixing ratio. This phenomenon is attributed to the stronger interaction between the SDS and the solid, as the electrostatic interaction between SDS and alumina is stronger than that of the hydrogen bonding between DM and alumina. Clearly this effect is more pronounced for mixtures that have smaller amounts of SDS.

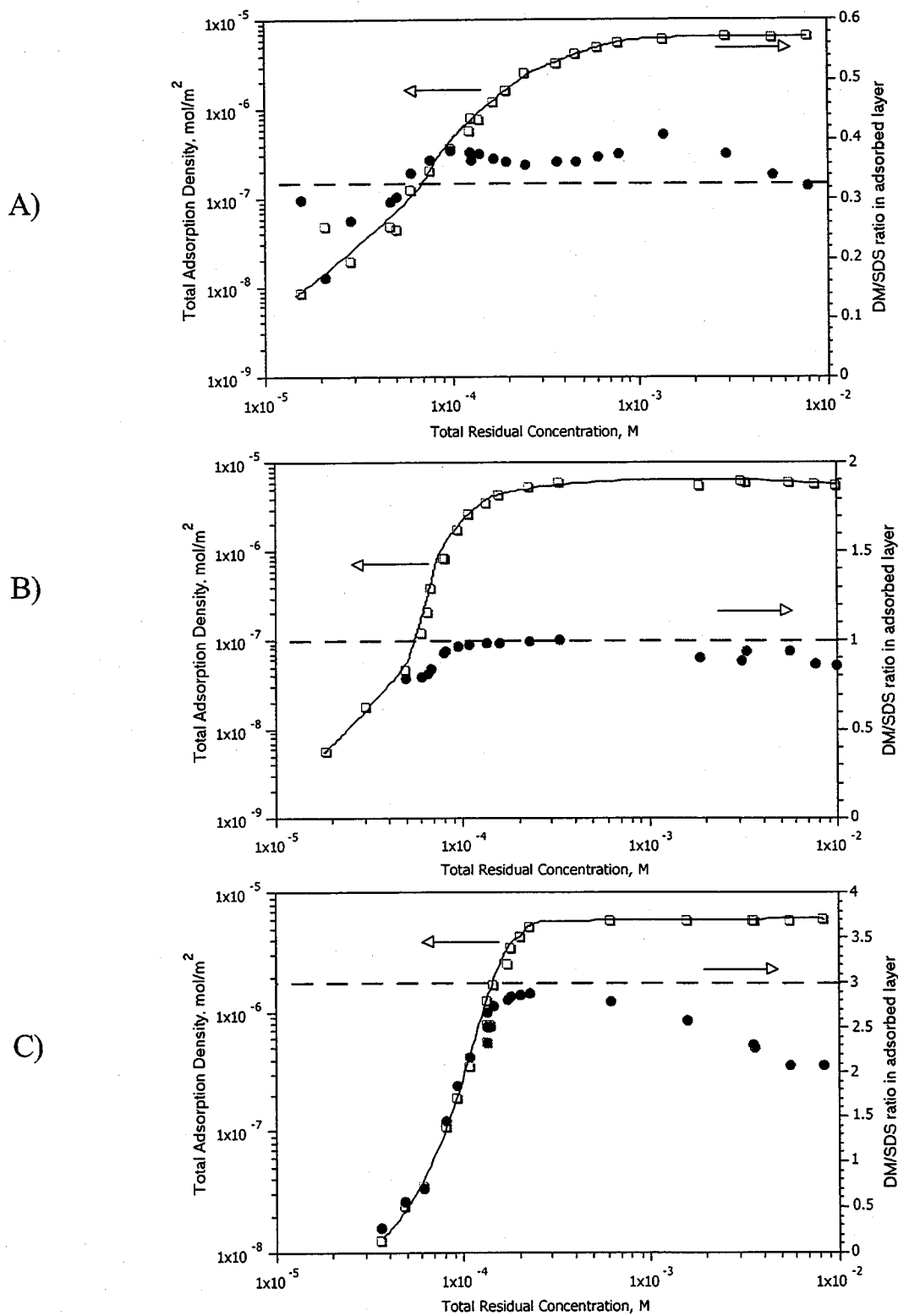


Figure 20. Adsorption of DM/SDS Mixtures and the DM/SDS ratios in the Adsorption Layer
 A) 1:3; B) 1:1; C) 3:1

3. Adsorption of dodecyl polyglucoside/sodium dodecylsulfate mixtures

The synergism for APG/SDS system can also be seen by comparing the adsorption of APG in the APG/SDS mixture with the adsorption of APG from its solution when present alone (Figure 21). The adsorption of APG from the mixture is markedly higher than that of APG from its single component solutions. At high concentrations, the adsorption of APG is lower because the surface is saturated.

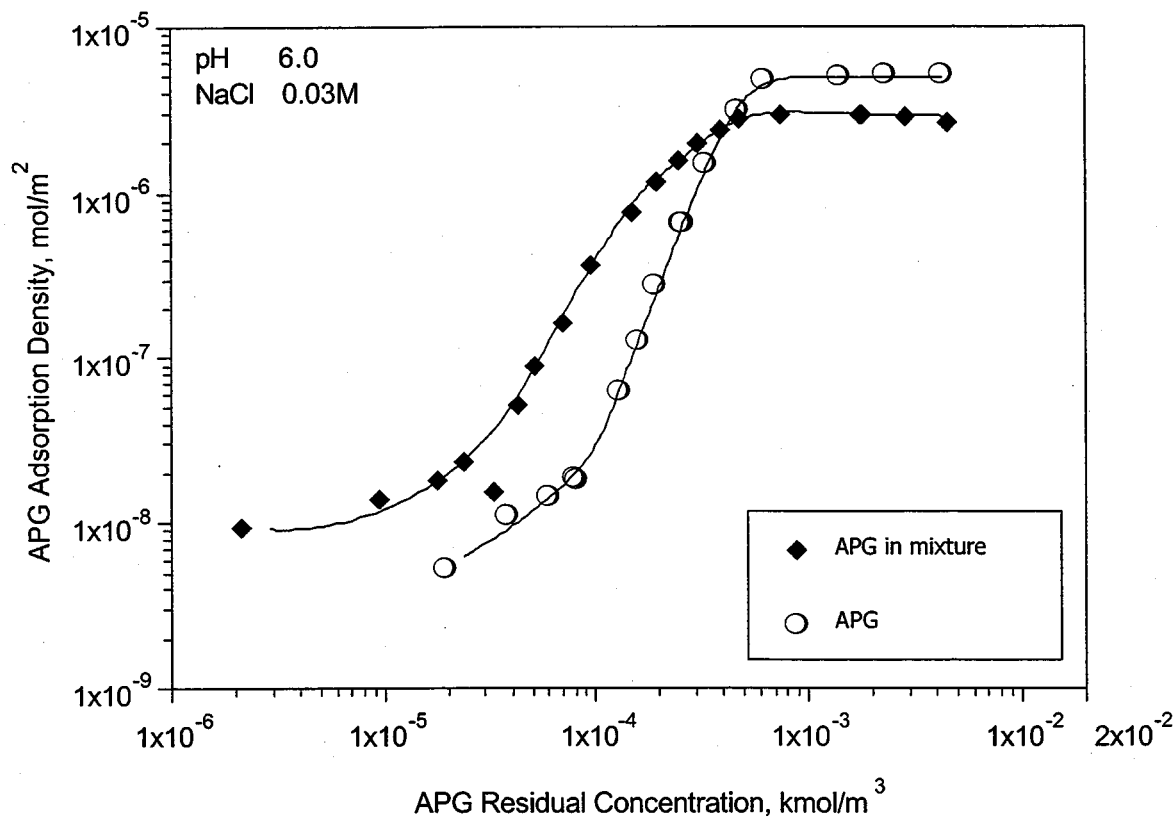


Figure 21. Adsorption of APG alone and from APG/SDS 1:1 Mixture on Alumina

The synergy for SDS can be observed by comparing the adsorption of SDS from the APG/SDS mixture with that from SDS alone in single component system (Figure 22). The adsorption of SDS from the mixture is much higher than SDS alone due to aggregation enhanced by the nonionic co-adsorbate, APG. In the plateau region, the adsorption density of SDS in the mixture is lower due to the competitive adsorption

with APG.

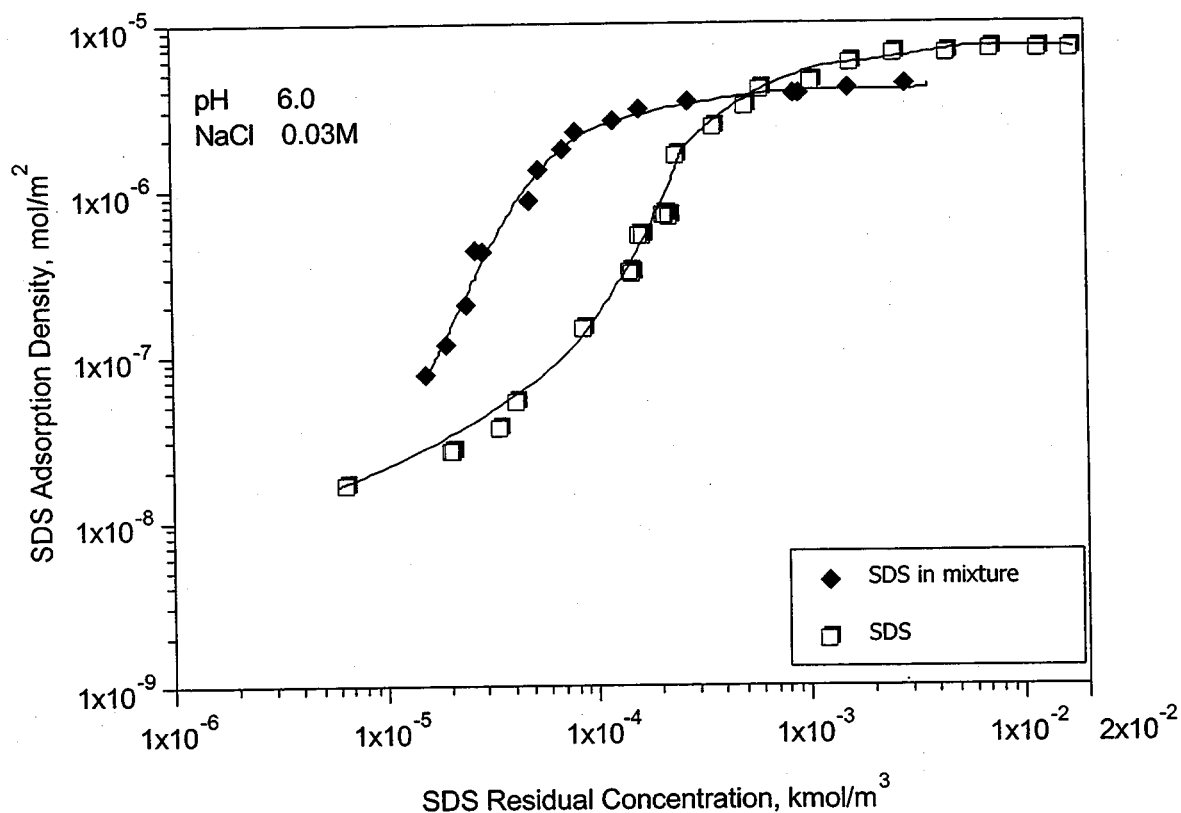


Figure 22. Adsorption of SDS alone and from APG/SDS 1:1 Mixture on Alumina

4. Summary of sugar-based surfactant/SDS mixtures adsorption at pH 6

In summary, the co-adsorption of n-dodecyl- β -D-maltoside (DM) and dodecyl polyglucoside with sodium dodecyl sulfate (SDS) on alumina was studied at pH 6 where alumina is positively charged. Marked synergistic effects between DM/APG and SDS were observed, especially in the region where hydrophobic chain-chain interaction dominates the adsorption process as long as the surface is not saturated. In the plateau region, clearly there is competition for adsorption sites. At this pH, SDS and DM/APG promote the adsorption of each other and there exists mainly synergism. The strongest synergism was found when the DM:SDS was 1:1.

III. Adsorption of Sugar-based Surfactants with Anionic Surfactant at pH 11

1. Adsorption of dodecyl polyglucoside/sodium dodecylsulfate and n-dodecyl- β -D-maltoside/sodium dodecylsulfate mixtures

Co-adsorption is examined under basic pH condition (pH 11) when the negatively charged sulfate adsorbs very little on alumina. The results obtained for the dodecyl polyglucoside/sodium dodecyl sulfate 1:1 mixture and n-dodecyl- β -D-maltoside/sodium dodecyl sulfate 1:1 mixture on alumina at pH 11 are illustrated in Figures 23 and 24. It is to be noted that at this pH, adsorption of negatively charged SDS on the similarly charged alumina is very low. The adsorption of the mixtures under these conditions is between that of DM/ C_{12} -APG and SDS, even when the surface is not fully covered by the surfactant. The presence of SDS in the system reduces the adsorption of the sugar-based surfactants under these conditions.

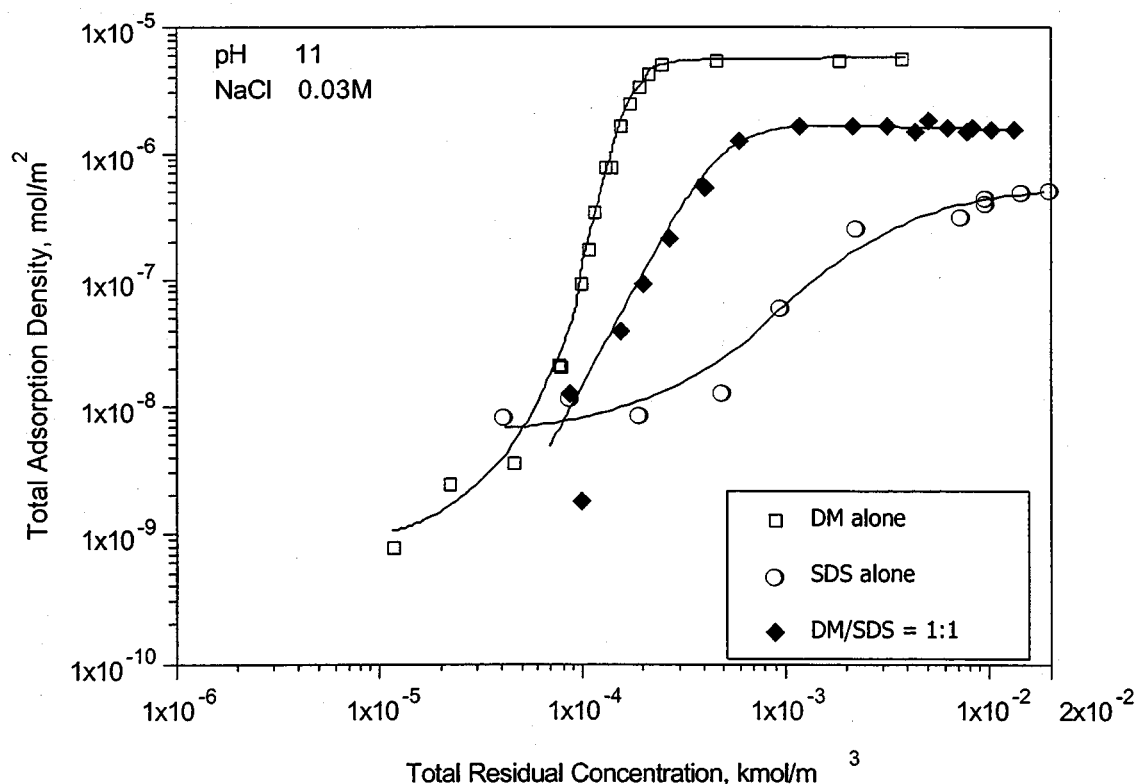


Figure 23. Adsorption of n-dodecyl- β -D-maltoside(DM), sodium dodecyl sulfate (SDS) and C_{12} -APG/SDS 1:1 Mixtures on Alumina at pH 11

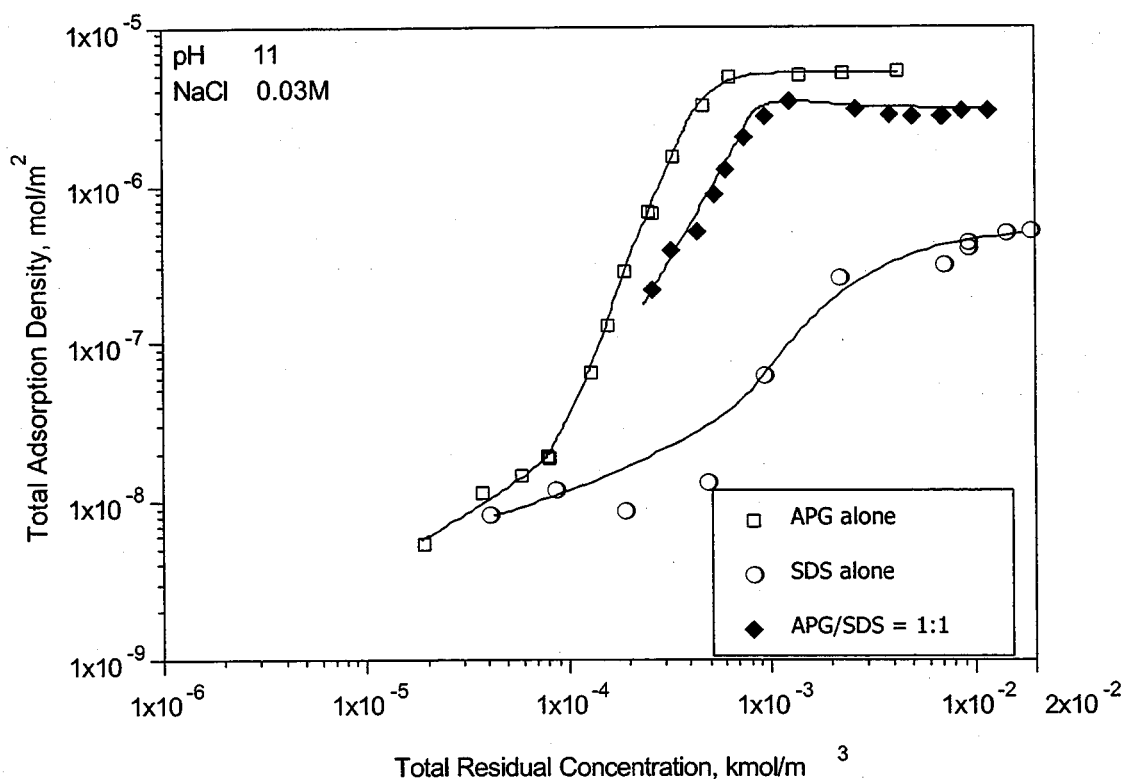


Figure 24. Adsorption of dodecyl polyglucosides(C12-APG), sodium dodecyl sulfate (SDS) and C₁₂-APG/SDS 1:1 Mixtures on Alumina at pH 11

The effect of n-dodecyl- β -D-maltoside (DM) and sodium dodecyl sulfate (SDS) mixing ratios on the adsorption of DM, SDS and their mixtures is illustrated in Figure 25 for 3:1, 1:1 and 1:3 ratios. The results show that more the SDS in the system, lower is the total adsorption density of the surface mixtures. Interestingly, there are antagonistic or competitive effects between SDS and DM under these conditions.

The adsorption of sodium dodecyl sulfate from SDS solution and from the DM/SDS mixtures on alumina is plotted in Figure 26 as a function of the residual SDS concentration. Adsorption of SDS from the mixtures is enhanced by the presence of DM except in the very high concentration regions. This is proposed to be due to the adsorbed DM functioning as anchor molecules for the SDS through hydrophobic chain-chain interactions. Thus at least for SDS, there are some synergistic effects in the surfactant mixtures with DM.

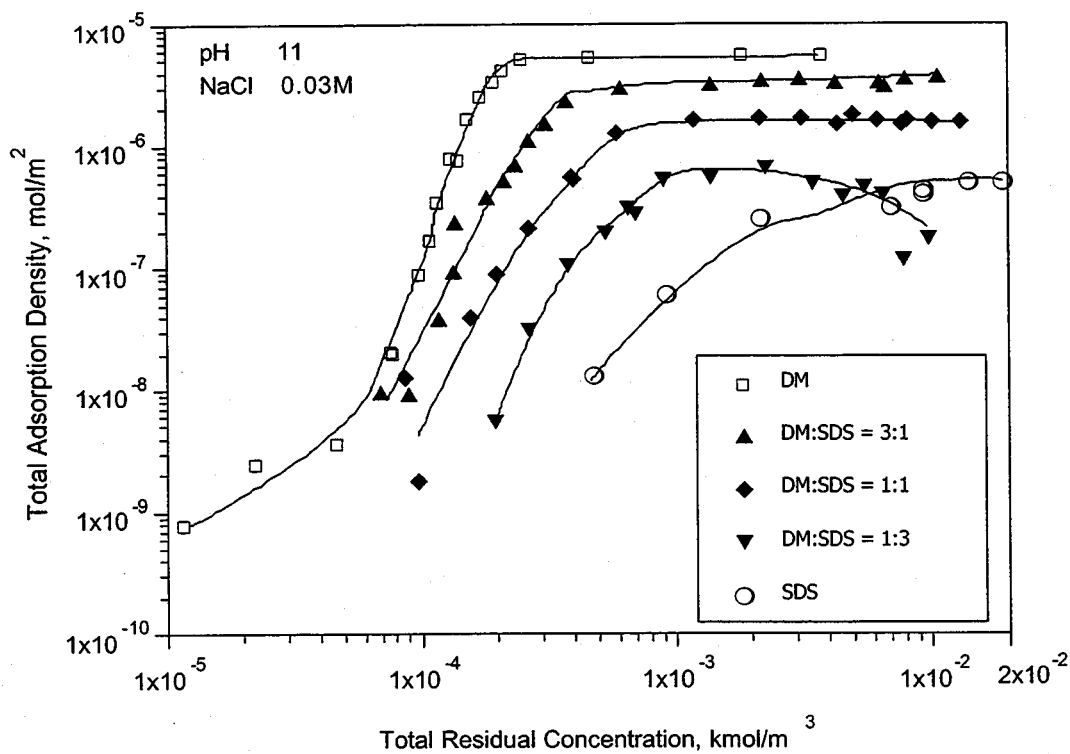


Figure 25. Adsorption of DM, SDS and their 3:1, 1:1 and 1:3 Mixtures on Alumina at pH 11

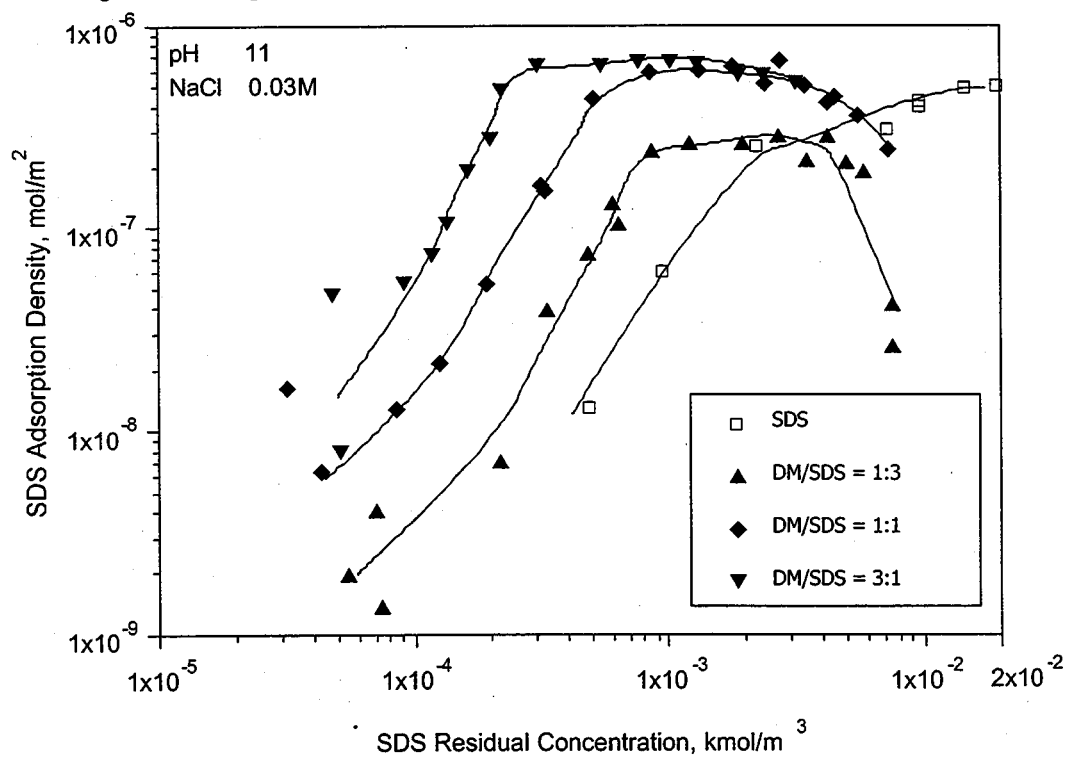


Figure 26. Adsorption of SDS on Alumina at pH 11: Adsorption for SDS alone and from DM/SDS 3:1, 1:1 and 1:3 Mixtures

In contrast to the above, it can be seen from Figure 27 that the DM adsorption is enhanced by SDS in the rising part but depressed in the plateau region. It can be seen from Figure 25 that the total adsorption of DM + SDS is decreased as SDS in the mixture increased. It can be concluded that in this system at pH 11, as a whole there are mainly antagonist effects between DM and SDS.

The same antagonism can be seen for the APG/SDS mixed system at pH 11 by comparing the adsorption of APG alone vs. that from the mixture (Figure 28), and adsorption of SDS alone vs. that from the mixture (Figure 29).

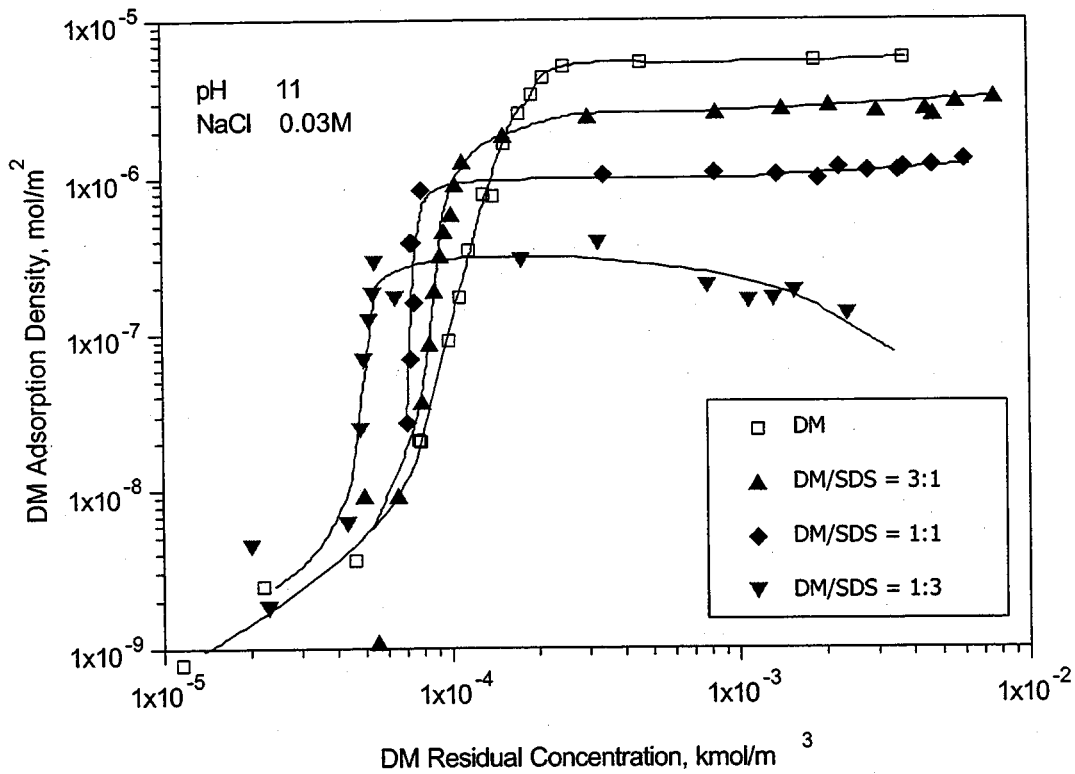


Figure 27. Adsorption of DM on Alumina at pH 11:
Adsorption for DM alone and from DM/SDS 3:1, 1:1 and 1:3 Mixtures

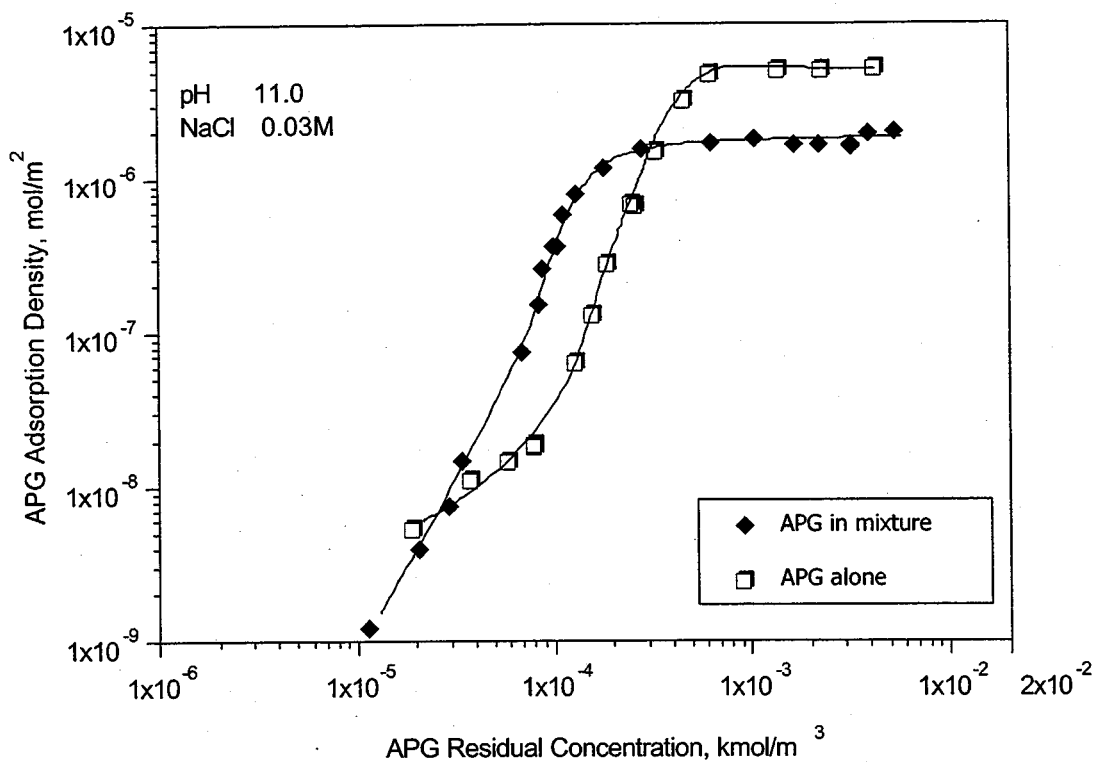


Figure 28. Adsorption of APG alone and in APG/SDS 1:1 mixture on alumina at pH 11

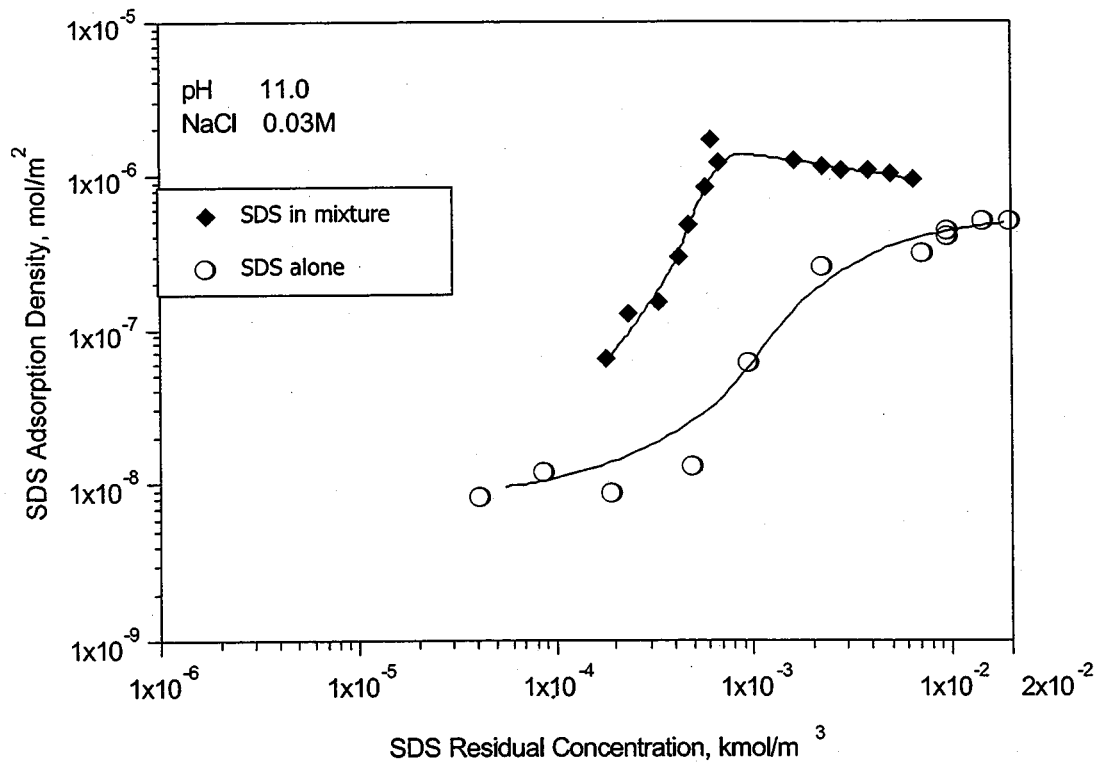


Figure 29. Adsorption of SDS alone and in APG/SDS 1:1 mixture on alumina at pH 11

2. Summary of sugar-based surfactant/SDS mixtures adsorption at pH 11

In summary, co-adsorption of sugar-based n-dodecyl- β -D-maltoside (DM) and dodecyl polyglucosides (C₁₂-APG) on alumina from their mixtures with anionic sodium dodecyl sulfate (SDS) was investigated at pH 11 where it is negatively charged. At this pH, the adsorption of APG/SDS, or DM/SDS mixture is less than those of APG or DM alone. The presence of SDS in the systems reduces the sugar-based surfactants adsorption except in the rising part of the isotherm, although the SDS adsorption is increased due to hydrophobic interaction with sugar-based surfactants. In general there is mainly antagonistic effects between n-dodecyl- β -D-maltoside (DM) and dodecyl polyglucosides (C₁₂-APG) with sodium dodecyl sulfate (SDS) at this pH.

V. Theoretical And Experimental studies of the Adsorption of Surfactant at Interfaces

1. Description Of The Model

When a clean interface is created in a surfactant solution, surfactant monomer adsorbs onto the surface from the sublayer of liquid immediately adjacent to the surface as a function of time. The adsorption reduces the monomer concentration in the subsurface region causing breakdown and diffusion of micelles from regions far away from the surface towards the surface. We examine the case in which the rate of micelle breakdown is much faster than the rate of its bulk diffusion towards the surface. This will be the case as long as the micelle concentration is not too large. In this case, micelles act as reservoir to maintain a monomer concentration equal to the CMC. Two regimes of surfactant transport are studied.

In the first, the initial kinetic rate of monomer adsorption is assumed to be very fast compared to the rate at which micelles diffuse from the bulk to the surface. Micellar diffusion cannot supply surfactant fast enough to the subsurface region to maintain concentration of the monomer at CMC, and as a result micelles disappear in the vicinity of the interface creating a micelle-free zone the front of which moves outward from the surface. At the front, micelles break down to supply surfactant monomers to the zone. Within the micelle free zone, monomer diffuses to the surface from the front where its value is equal to the CMC and where the sublayer concentration is controlled by the kinetic quasi-equilibrium and is below the CMC. From the front of the micelle free zone to the region of the solution far from the interface, the monomer concentration is uniform. In this region, micelles diffuse from the far field (where the micelle concentration is prescribed) to the front (where the micelle concentration is zero) to replenish micelles breaking down at the front. As adsorption onto the surface proceeds, the monomer subsurface concentration increases towards the CMC, the concentration gradient of monomer across the micelle-free zone is reduced and the front begins to move back towards the interface. The micelle diffusion gradient also relaxes as the monomer flux in the micelle free zone decreases. At equilibrium, the front arrives back at the interface and the bulk solution is once again a uniform micellar solution.

In the second regime, the initial rate of adsorption is assumed to be of the same order as the rate of micellar diffusion. Micellar diffusion can now supply enough micelles to the surface vicinity so that the micellar breakdown maintains a value of the monomer concentration equal to the CMC for an extended period. During this time the micelle concentration in the subsurface layer decreases so that diffusion of micelles can continue to match the kinetics of adsorption of surfactant onto the surface. Eventually, the micelle concentration at the sublayer falls to zero, and diffusion of micelles can no longer match the kinetics of adsorption. A micelle free zone once again forms as before, and the front of the zone moves outward and eventually returns to the surface at equilibrium. Numerical solutions of the dynamic surface concentration are obtained for both cases in terms of kinetic coefficients and monomer and micelle diffusion coefficients. By using an equation of state, the surface tension reduction accompanying the adsorption is calculated. Micelle diffusion coefficients and the number of monomers per micelle are known from light scattering experiments, and monomer diffusion coefficients and adsorption kinetics parameters are known from measurements of dynamic tension reduction for solutions below the CMC. As a result this micelle transport model can predict the adsorption (and tension reduction via the equation of state) with no adjustable parameters.

2. Mathematical Formulation

At $t=0$, a fresh interface is created and monomers begin to adsorb at the fresh interface. The Columbia model is for a flat interface that extends infinitely in the x-y direction and is located at $z=0$. The bulk fluid is assumed to extend infinitely in the z direction. The adsorption of the monomers is balanced by the breakup of the micelles that diffuse from the bulk. Let c_m and c be the concentration of micelles and monomers respectively. The diffusion of both species is governed by the diffusion equation:

$$\frac{\partial c}{\partial t} = D \frac{\partial^2 c}{\partial z^2}$$

$$\frac{\partial c_m}{\partial t} = D_m \frac{\partial^2 c_m}{\partial z^2}$$

The initial conditions are :

$$c(z, 0) = \text{CMC}$$

$$c_m(z, 0) = c_b$$

The boundary conditions are:

at $z = 0$

$$\frac{\partial \Gamma}{\partial t} = \beta(\Gamma_\infty - \Gamma)C_s - a\Gamma$$

$$D \frac{\partial c(0, t)}{\partial z} = \beta(\Gamma_\infty - \Gamma)C_s - a\Gamma$$

at $z = \delta(t)$

$$D \frac{\partial c(d(t), t)}{\partial z} = ND_m \frac{\partial c_m(d(t), t)}{\partial z}$$

$$C_M(\delta(t), t) = 0$$

$$C(\delta(t), t) = \text{cmc}$$

at $z = \infty$

$$C_M(\infty, t) = c_b$$

3. Experiments

The surface tension experiments were done using a sessile bubble apparatus at room temperature of 25°C. Figures 30 through 34 show the surface tension of a $C_{14}E_6$ solution as a function of time; The critical micelle concentration of $C_{14}E_6$ is 9.19×10^{-6} M. In figure 30, the surfactant concentration is 5.965×10^{-6} M which is slightly below the CMC; this concentration was used for the purpose of comparing with data previously obtained by other researchers and for checking our apparatus and solution. As shown in the plot, the surface tension starts at 72 mN/m which is the surface tension of a clean air-water interface

and reduces to an equilibrium tension of 32 mN/m in about 400 seconds. In figure 31, the bulk concentration of $C_{14}E_6$ is 1.927×10^{-5} M which is approximately twice the CMC; at this concentration, the tension drops to 31 mN/m in 140 seconds. Since the bulk concentration at the beginning of the experiment is higher than the CMC and the depletion in the bulk concentration due to adsorption is negligible, the bulk concentration stays above the CMC even after the equilibrium has been reached. In our model, since there is no micelle adsorption on the interface, at equilibrium the adsorption of monomers is balanced by

desorption, i.e., $\Gamma = \Gamma_{\infty} \frac{\beta \text{CMC}}{\beta \text{CMC} + \alpha}$. Thus, a further increase in the bulk concentration should not

affect the equilibrium surface concentration and surface tension. However, the time needed to reduce the tension from that of a clean interface to the equilibrium value will decrease. The model predictions are supported by the experimental data in figures 32 through 34. The bulk concentration in figure 32 is 3.911×10^{-5} M which is about 4 times the CMC. As shown in the plot, the equilibrium tension is still 31 mN/m; however, the time needed to reach the equilibrium is about 60 seconds. At a concentration of 7.719×10^{-5} M, approximately eight times the CMC, it takes 20 seconds to reach the equilibrium and at a concentration of 9.666×10^{-5} , approximately ten times the CMC, it takes 14 seconds to attain the equilibrium. These results are summarized in the following table:

Table 4. Summary of Figures 30 - 34

Concentration [M]	Equilibrium Surface Tension [mN/m]	Time [seconds]
5.965×10^{-6} (below CMC)	32	400
1.927×10^{-5}	31	140
3.911×10^{-5}	31	60
7.719×10^{-5}	31	20
9.666×10^{-5}	31	14

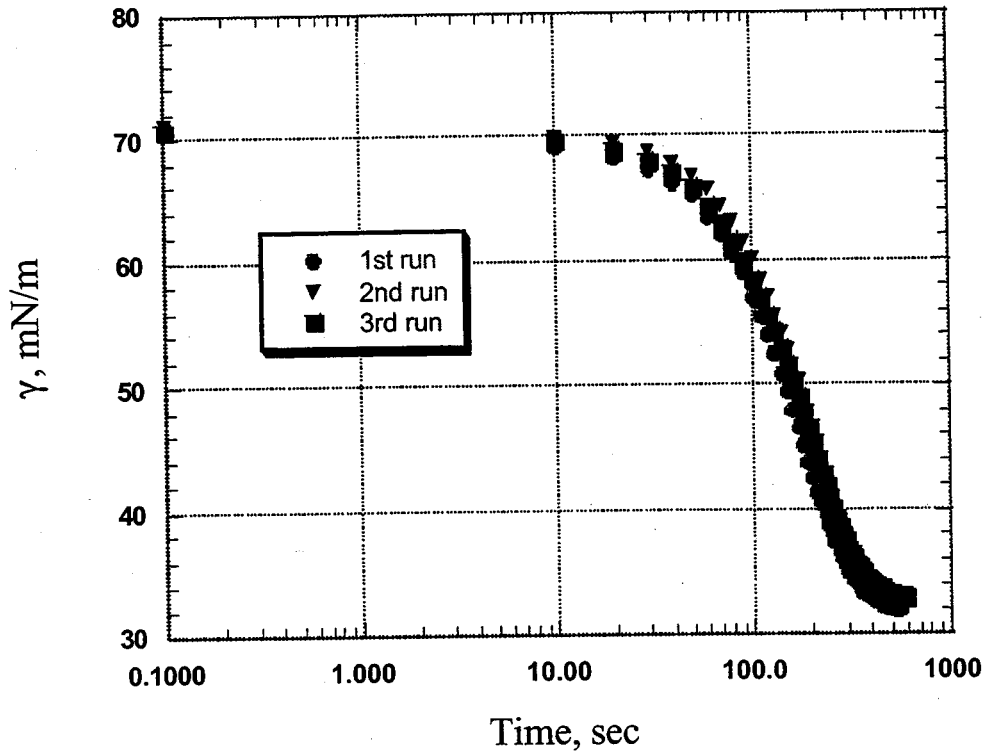


Figure 30 Surface tension of $C_{14}E_6$ solution ($5.965 \times 10^{-6} M$) as a function of time

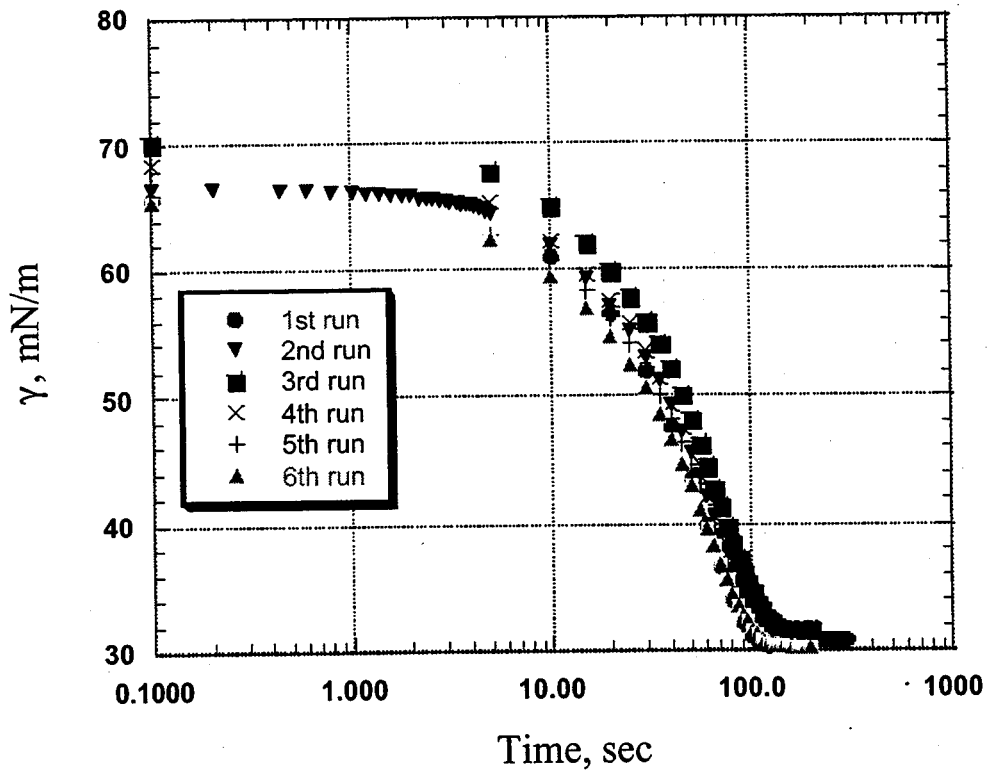


Figure 31 Surface tension of $C_{14}E_6$ solution ($1.927 \times 10^{-5} M$) as a function of time

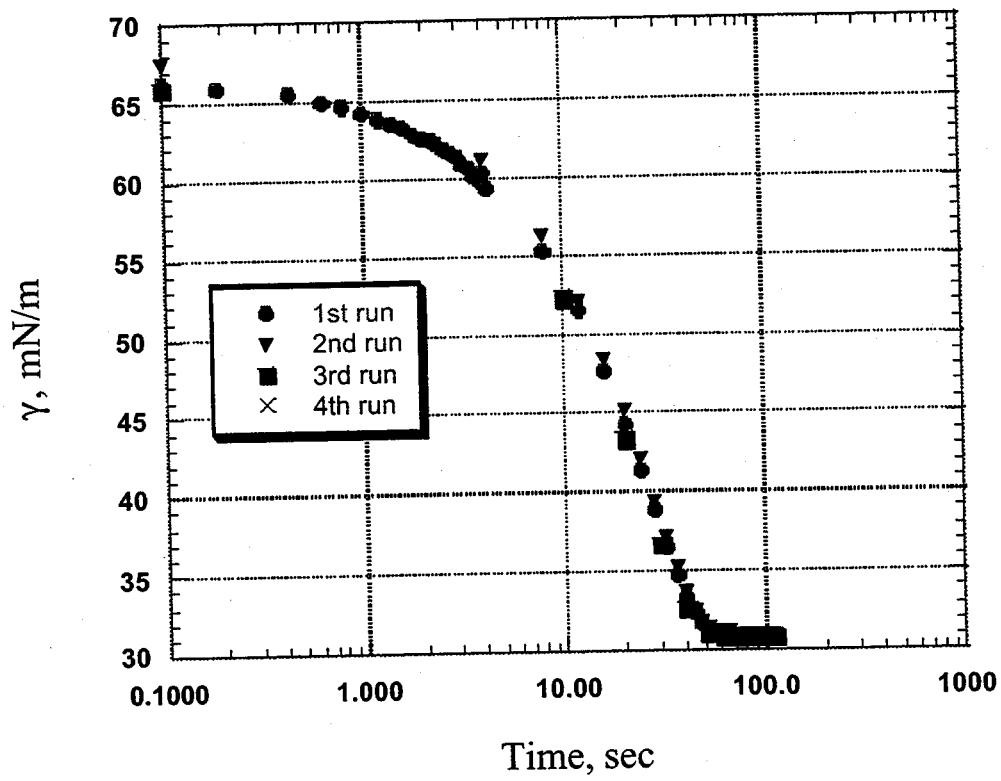


Figure 32 Surface tension of $C_{14}E_6$ solution ($3.911 \times 10^{-5} M$) as a function of time

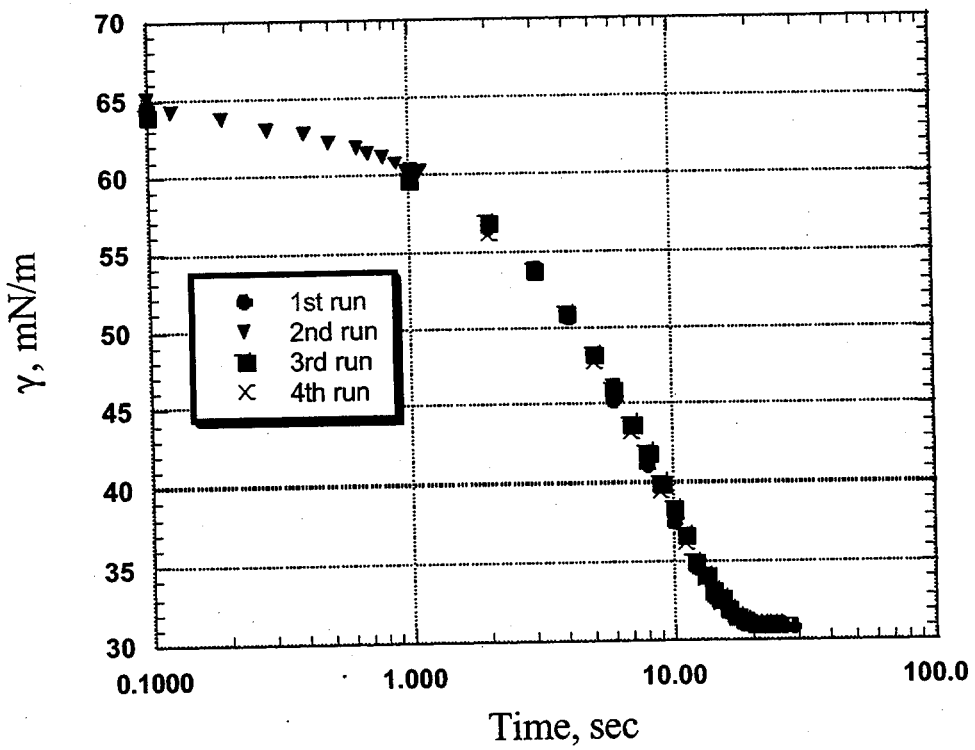


Figure 33 Surface tension of $C_{14}E_6$ solution ($7.719 \times 10^{-5} M$) as a function of time

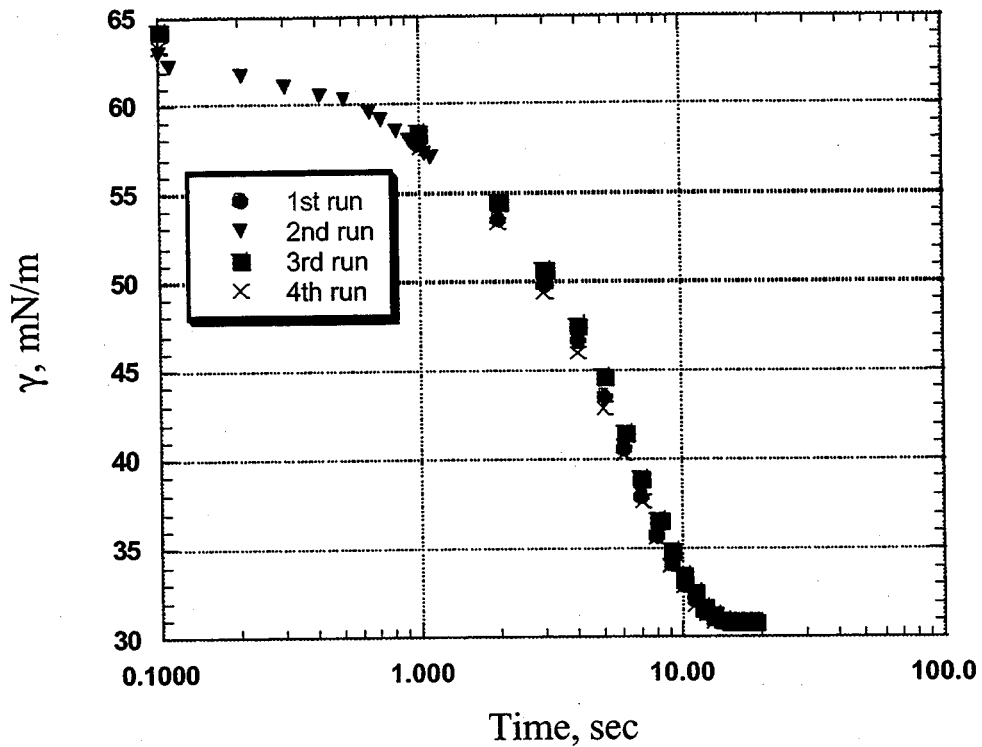


Figure 34 Surface tension of $C_{14}E_6$ solution ($9.666 \times 10^{-5}M$) as a function of time

It is clear from these results that a valid theoretical model can be developed for surfactant adsorption. The model will indeed need modifications for it to be applicable to real conditions involving mixed micelles and solid particles.

Publications and Presentations

1. *Brian A. Pethica, Zhenghe Zhu, Anjing Lou and P. Somasundaran*, "Surface and Colloidal Properties of Cyclic Amides. 4. N-cyclohexyl-2-pyrrolidone/water Mixtures Aggregation in solution and adsorption at the air/solution interface" Submitted to Journal of Colloid and Interface Science.
2. P. Somasundaran and L. Huang, "Adsorption/aggregation of Surfactants And Their Mixtures at Solid-liquid Interfaces" *Advances in Colloid and Interface Science*, Vol. 88. P. 179-208, 2000
3. P. Somasundaran and L. Huang, "Adsorption of Polymers at Solid-liquid Interfaces" Submitted for the book entitled "Polymer in Personal Care, Pharmaceutical, and Industrial Application", To be published by Marcel Dekker Inc..
4. S. Hazair, P. Somasundaran, C. Maldarelli, "Model for Dynamic Surface Tension above the Critical Micelles Concentration" AICHE Meeting presentation, Los Angeles, Nov. 2000

